Molecular Biology of the Cell
Vol. 19, 2193–2207, May 2008

Genome-wide Expression Profiling, In Vivo DNA Binding Analysis, and Probabilistic Motif Prediction Reveal Novel Abf1 Target Genes during Fermentation, Respiration, and Sporulation in Yeast

Ulrich Schlecht,*† Ionas Erb,* Philippe Demougin,* Nicolas Robine,‡§ Valérie Borde,‡ Erik van Nimwegen,* Alain Nicolas,‡ and Michael Primig*‖

*Biozentrum and Swiss Institute of Bioinformatics, CH-4056 Basel, Switzerland; ‡Centre National de la Recherche Scientifique Unité Mixte de Recherche 7147 Recombination and Genome Instability, Institut Curie, Université Pierre et Marie Curie, F-75248 Paris, France; and §Service de Bioinformatique, Institut Curie, F-75248 Paris, France

Submitted December 19, 2007; Revised February 14, 2008; Accepted February 19, 2008
Monitoring Editor: Mark Solomon

The autonomously replicating sequence binding factor 1 (Abf1) was initially identified as an essential DNA replication factor and later shown to be a component of the regulatory network controlling mitotic and meiotic cell cycle progression in budding yeast. The protein is thought to exert its functions via specific interaction with its target site as part of distinct protein complexes, but its roles during mitotic growth and meiotic development are only partially understood. Here, we report a comprehensive approach aiming at the identification of direct Abf1-target genes expressed during fermentation, respiration, and sporulation. Computational prediction of the protein's target sites was integrated with a genome-wide DNA binding assay in growing and sporulating cells. The resulting data were combined with the output of expression profiling studies using wild-type versus temperature-sensitive alleles. This work identified 434 protein-coding loci as being transcriptionally dependent on Abf1. More than 60% of their putative promoter regions contained a computationally predicted Abf1 binding site and/or were bound by Abf1 in vivo, identifying them as direct targets. The present study revealed numerous loci previously unknown to be under Abf1 control, and it yielded evidence for the protein's variable DNA binding pattern during mitotic growth and meiotic development.

INTRODUCTION

Progression through the mitotic and meiotic cell cycles in budding yeast is in part controlled by underlying expression programs that coordinate timing of induction with time of function of many genes essential for these processes (for review, see Futcher, 2002; Schlecht and Primig, 2003). Transcriptional control requires a complex interplay between activators and repressors, basal transcription factors, and enzymes involved in chromatin modification together with general regulatory factors such as Abf1. This protein was initially shown to be required for normal activity of autonomously replicating sequence (ARS) elements by direct interaction with its specific DNA binding motif (Rhode *et al.*, 1992). Subsequent studies revealed its contribution to mitotic and meiotic promoter activities via mutational analysis of its N-terminal DNA binding module, its C-terminal protein interaction domains, and its DNA target site (Kovari and Cooper, 1991; Cho *et al.*, 1995; Gailus-Durner *et al.*, 1996; Ozsarac *et al.*, 1997; Miyake *et al.*, 2002). The precise mechanism of action of Abf1 is not known, but its association with DNA has an effect on nucleosome positioning (Lascaris *et al.*, 2000; Yarragudi *et al.*, 2004). Exchanging Abf1-dependent regulatory elements in promoters mediating early and middle meiotic transcriptional activation suggested a role for the protein in enhancing gene expression to wild-type levels during spore development rather than controlling timing of induction (Pierce *et al.*, 1998).

Abf1 was proposed to be a hub protein that is part of many distinct protein complexes (Luscombe *et al.*, 2004). Direct physical interaction or coprecipitation was demonstrated for proteins likely involved in Abf1 phosphorylation (Cka1/Cka2 and Ckb1/Ckb2), nuclear localization (Pse1), SUMOylation (Smt3), and ARS binding activity (Cdc6). Other studies found the protein to coprecipitate with factors required for chromatin assembly and chromatin remodeling (Hta2, Htb1, Rvb1, Rvb2, and Isw2), transcriptional regulation (Mot1, Sth1, and Taf5), activity of RNA polymerase I (Hmo1 and Rpc40) and III (Rpc34, Rpc53, and Rpo31),

This article was published online ahead of print in *MBC in Press* (http://www.molbiolcell.org/cgi/doi/10.1091/mbc.E07–12–1242) on February 27, 2008.

Present addresses: † Stanford Genome Technology Center, 855 California Ave., Palo Alto, CA 94304; ‖ Institut National de la Santé et de la Recherche Médicale Unité 625, Université de Rennes 1, F-35042 Rennes, France.

Address correspondence to: Michael Primig (michael.primig@rennes.inserm.fr).

Author contributions: U.S. designed and performed research and analyzed data. I.E. and E.v.N. provided binding site predictions and analyzed data. P.D. produced the microarray data. N.R. and V.B. supported ChIP-Chip data production and provided analysis procedures. A.N. designed research. M.P. designed research, interpreted data, and wrote the paper.

© 2008 by The American Society for Cell Biology

Supplemental Material can be found at:
http://www.molbiolcell.org/content/suppl/2008/02/26/E07-12-1242.DC1

mRNA export from the nucleus (Yra1), and nucleotide excision repair (Rad7 and Rad16) (see BioGRID for references; Stark *et al*., 2006).

Genome-wide DNA binding assays and protein–protein interaction analyses have shown that Abf1 binds to a large number of promoters during mitotic growth and that it controls coregulated protein clusters (also termed "regulonic complexes" (Zhang *et al*., 2005) involved for example in cytoplasmic transport and histone deacetylation (Tan *et al*., 2007). Some of these Abf1-dependent clusters, such as motor proteins, seem to be conserved between yeast and fly (Tan *et al*., 2007). Dynamic network analysis covering multiple conditions revealed that Abf1 controls cell growth and in addition regulates intracellular transport during stress response, indicating that it can activate distinct target genes when cells are exposed to different environmental cues (Luscombe *et al*., 2004). The correlation between its role as a transcriptional regulator and its DNA binding activity, as assessed by chromatin immunoprecipitation in combination with microarrays (ChIP-Chip) or protein binding microarrays is unclear because many promoters that are bound do not seem to contain a match to the target site. In contrast, a statistical model of the sequence-dependent binding energy of Abf1, which is similar to the position-specific weight matrix model used in this study, is in good agreement with in vitro and in vivo binding data (Kinney *et al*., 2007, and references therein). Recently, the temperature-sensitive *abf1-1* allele was used to identify target genes in mitotically growing haploid cells by using microarrays because the mutant protein fails to interact with its target site at the restrictive temperature due to a point mutation in the DNA binding domain (Rhode *et al*., 1992; Miyake *et al*., 2004; Yarragudi *et al*., 2007). However, these studies lacked wild-type and mutant controls at the permissive temperature, they failed to include growth in the absence of a fermentable carbon source, and they did not cover meiotic development.

In this article, we report the results of a comprehensive approach to studying the role of Abf1 in controlling mitotic growth during fermentation, respiration, and sporulation. We first characterized the growth properties of diploid wild-type versus mutant yeast cells containing one or two *abf1-1* alleles at the permissive (25°C), semipermissive (30°C), and restrictive (37°C) temperatures on solid and in liquid growth media containing glucose (YPD) or acetate (YPA). Subsequently, the ability of diploid yeast cells containing one wild-type or *abf1-1* temperature-sensitive mutant allele to form spores was monitored using plate and liquid sporulation assays carried out at temperatures that permit (25, 28, and 33°C) or inhibit (37°C) sporulation. To identify mitotic and meiotic genes under direct transcriptional control of Abf1, a combination of computational target site prediction, a genome-wide DNA binding assay of mitotic and meiotic cells, and expression profiling of wild-type versus mutant strains was used. Obtaining results from three complementary methods enabled us to set optimally low filtration thresholds for each data type, to allow for efficient mitotic and meiotic target gene discovery. The microarray expression profiling and binding data are available for downloading via the certified public ArrayExpress repository at the European Bioinformatics Institute (Parkinson *et al*., 2005). A graphical display in the context of genome annotation is accessible via the Internet through the GermOnline database (http://www.germonline.org/) (Gattiker *et al*., 2007).

MATERIALS AND METHODS

Yeast Culture Conditions

Diploid W303 wild-type and *abf1-1* mutant strains (Table 1) were grown in YPD (1% yeast extract, 2% bactopeptone, and 2% glucose) or YPA (1% yeast extract, 2% bactopeptone, and 1% potassium acetate) at 25°C to a density of 2×10^7 cells/ml. The cultures were split and incubated either at 37 or 25°C first in a water bath and subsequently in a rotatory shaker at 37°C (260 rpm). Cells were harvested after 60 min, washed with sterile water, snap-frozen in liquid nitrogen, and stored at −80°C. Diploid W303 strains containing one wild-type or mutant allele were sporulated in SPII (2% acetate, pH 7.0) at 28°C for 5 and 9 h, respectively, and then kept at 28, 33, or 37°C for 1 h before harvesting, washing, and storing at −80°C. A diploid SK1 strain was grown and sporulated using standard conditions (Hochwagen *et al*., 2005), and 50-ml samples were taken for a genome-wide DNA binding assay in YPD, YPA, and SPII 4 and 8 h after initiation of meiosis.

Antibodies

Rabbit antibodies were raised against His6-Abf1 (amino acids 264–513) affinity purified from a bacterial extract by using XL10-GOLD (Stratagene, La-Jolla, CA). The final bleed was aliquoted, snap-frozen, and stored at −80°C. The commercial hemagglutinin (HA) antibody 12CA5 (Roche Diagnostics, Mannheim, Germany) was used to detect HA_3-tagged Abf1 protein. Commercial Abf1 antibodies were obtained from Santa Cruz Biotechnology (Santa Cruz, CA).

Western Blotting

Protein extracts were prepared using acid-washed glass beads and a BeadBeater apparatus (BioSpec, Bartlesville, OK). Three cycles of bead beating were done at maximal intensity for 30 s. Extracts were kept on ice for 2 min

Table 1. Yeast strains

Strain	Genotype	Reference
KM7	*MAT*a leu2-3 his4-519 ade1-100 ura3-52 GAL-*ABF1*::*URA3*	Gonçalves *et al*. (1992)
JCA30	W303 *MAT*a trp1 Δ his3Δ200 ura3-52 lys2-801 ade2-1 gal *ABF1 HIS3*	Rhode *et al*. (1992)
JCA31	W303 *MAT*a trp1 Δ his3Δ200 ura3-52 lys2-801 ade2-1 gal abf1-1 *HIS3*	Rhode *et al*. (1992)
JCA40	W303 *MATα* trp1 Δ his3Δ200 ura3-52 lys2-801 ade2-1 gal *ABF1 HIS3*	Rhode *et al*. (1992)
JCA41	W303 *MATα* trp1 Δ his3Δ200 ura3-52 lys2-801 ade2-1 gal abf1-1 *HIS3*	Rhode *et al*. (1992)
MPY170	SK1 *MAT*a/α ho::LYS2 ura3 lys2 leu2::hisG arg4-Nsp/arg4-Bgl his4x::*LEU2-URA3*/his4B::*LEU2*	Primig *et al*. (2000)
MPY284	*MAT*a/α trp1Δ/trp1Δ his3Δ200/his3Δ200 ura3-52/ura3-52 lys2-801/lys2-801 ade2-1/ade2-1 gal/gal *ABF1/ABF1*	This study
MPY283	*MAT*a/α trp1Δ/trp1Δ his3Δ200/his3Δ200 ura3-52/ura3-52 lys2-801/lys2-801 ade2-1/ade2-1 gal/gal abf1-1/abf1-1	This study
MPY285	MPY283 pRS416-*ABF1*	This study
MPY125	*MAT*a/α trp1Δ/*TRP1* his3Δ200/his4-519 ura3-52/ura3-52 ade2-1/ade1-100 gal *ABF1*/GAL-*ABF1*::*URA3*	This study
MPY128	*MAT*a/α trp1Δ/*TRP1* his3Δ200/his4-519 ura3-52/ura3-52 ade2-1/ade1-100 gal abf1-1/GAL-*ABF1*::*URA3*	This study
USY368	MPY284 *CDC3/CDC3-eGFP*	This study
USY364	MPY285 *CDC3/CDC3-eGFP*	This study

between each cycle. The concentration of protein extracts was adjusted to 15 μg/μl. For electrophoretic analysis, 60 μg of protein extract was loaded onto a 10% SDS gel run at 100 V for 2 h in the cold room. Western blotting was performed using standard conditions and nitrocellulose membranes pretreated with 3% milk in 0.1% phosphate-buffered saline (PBS)-Tween and then washed in 0.1% PBS-Tween. The secondary anti-rabbit immunoglobulin G antibody was diluted 1:20,000 (Sigma-Aldrich, Paris, France). The enhanced chemiluminescence kit was used to reveal Western blot signals (Bio-Rad, Hercules, CA).

Immunofluorescence

To visualize nuclei and Cdc3-green fluorescent protein (GFP), cells were fixed for 1 h in 3.7% formaldehyde in growth media, washed once in 1× PBS, and resuspended in a 5 μg/ml solution of Hoechst dye (Invitrogen, Carlsbad, CA). Cells were incubated for 30 min at room temperature, and then they were washed three times in 1× PBS. Cells were analyzed using an Axioplan 2 imaging microscope (Carl Zeiss, Jena, Germany) equipped with a Plan Neofluar 100× Ph3 numerical aperture 1.3 objective. Digital images were produced with a TE/CCD-1000PB camera (Princeton Scientific Instruments, Monmouth Junction, NJ). The excitation intensity was controlled with different neutral density filters (Chroma Technology, Brattleboro, VT).

Electrophoretic Mobility Shift Assay (EMSA)

Probe annealing, labeling, and the binding reaction were done as described previously (Primig *et al*., 1991, 1992). Antibody supershift assays were carried out using diluted antisera that were added to the probe–protein mix for 5 min before loading on a 6% polyacrylamide gel (0.5× Tris-EDTA) run at room temperature for 120 min at 200 V. Gels were dried and analyzed using a PhosphorImager Storm 860 (GE Healthcare, Little Chalfont, Buckinghamshire, United Kingdom).

Computational Binding Site Prediction

For each intergenic region in *Saccharomyces cerevisiae*, orthologous intergenic regions from the four other budding yeast species were obtained using the open reading frame (ORF) annotations from Kellis *et al*. (2003) and Cliften *et al*. (2003), and all groups of orthologous intergenic regions were aligned with T-Coffee (Notredame *et al*., 2000). The phylogenetic tree of the species was reconstructed using third positions of fourfold degenerate codons in orthologous genes. A weight matrix was reconstructed by simultaneously clustering and aligning known Abf1 sites from the SCPD collection (Zhu and Zhang, 1999). We then predicted binding sites in all intergenic region alignments by using the MotEvo algorithm (Erb and van Nimwegen, 2006). Briefly, MotEvo finds all intergenic sequence segments in the *S. cerevisiae* reference genome that match the weight matrix better than a third order Markov model of background intergenic sequences. It then collects the corresponding sequence segments from the other species from the alignment. Each of these segments is first scored under the weight matrix and a species-dependent background model and those orthologous segments that score better under the weight matrix are marked as "under selection." The probability of the observed sequence alignment is calculated under an evolutionary model that assumes all sequences under selection were constrained to retain their match to the weight matrix, by using the inferred phylogenetic tree. This probability is then compared with the probability of the observed alignment under background evolution, and under evolution that is constrained by a different (unknown) selective pressure, to obtain a posterior probability for the site. The positional profile was generated by summing the posterior probabilities of all binding sites that occur upstream of a single gene (i.e., excluding divergently transcribed regions) for which a transcription start site has been determined in Zhang and Dietrich (2005).

Comparison of the Methods for Genome-Wide Abf1 Target Identification

To determine the log-odds ratios of site occurrence, we combined, for each intergenic region, the posterior probabilities of all sites to calculate the probability p that at least one true site occurs. The log-odds ratio r is then given by $r = \log(p/(1 - p))$. The log-odds ratios for each intergenic region to be bound by Abf1 were determined from the ChIP-Chip data as follows. First, probes were mapped to the intergenic regions: a probe was considered to belong to a region if at least 80% of its sequence was contained in the region. Usually, several probes mapped to one region. Using the log-ratio of binding at each probe we calculated, for each region, the probability that binding occurred at least one probe in the region. The final probability of binding p is given by the taking the maximum of this probability over all experiments. The log-odds ratio r is then given by $r = \log(p/(1 - p))$. For each experiment the noise in the expression changes of both wild-type and mutant was estimated from the variance of the duplicate measurements to calculate z-statistics. For each gene, the z-statistic was given by the difference in the observed expression change in mutant and wild-type, relative to the estimated noise, summed over all experiments. To assign z-statistics to intergenic regions, the maximal z-value of the two downstream genes was taken for divergently transcribed regions. We thus obtained, for each intergenic region, a log-odds ratio for site occurrence, a log-odds ratio for binding, and a z-statistic for expression change. A set of cut-off values for the three variables partitions the intergenic regions into eight groups, varying from "unregulated" according to all three methods to "regulated" by all three methods. The overall agreement of the three methods was calculated by the mutual information in the partition into eight groups. We calculated the fractions $f(x,y,z)$ of regions in each of the eight groups whereby x, y, and z were either 0 (unregulated) or 1 (regulated). The mutual information of the partition is then given by

$$I = \sum_{x,y,z} f(x,y,z) \log\left[\frac{f(x,y,z)}{f_s(x) f_b(y) f_e(z)}\right]$$

where $f_s(1)$ is the overall fraction of regions with binding site predictions over the cut-off, $f_b(1)$ the fraction of regions with binding over the cut-off, and $f_b(1)$ the fraction of regions with expression change over the cut-off. We then determined the combination of cut-offs for the three methods that maximized the mutual information I. We also calculated the mutual information (at the optimal cut-offs) for each pair of methods.

Chromatin Immunoprecipitation

Cultures (20 ml) containing ~4×10^8 cells were treated with 1% formaldehyde for 15 min at room temperature. DNA was processed and analyzed by semiquantitative polymerase chain reaction (PCR) as described previously (Borde *et al*., 2004).

ChIP-Chip Assay

DNA was eluted from the protein G beads, purified, amplified, and labeled as described previously (Borde *et al*., 2004). Hybridization was carried out using spotted microarrays containing yeast ORFs and intergenic regions as described in Robine *et al*. (2007). Spotted probes were assigned to promoters as in (Lee *et al*., 2002), a reference table is available for downloading from http://staffa.wi.mit.edu/cgi-bin/young_public/navframe.cgi?s = 17&f = downloaddata.

ChIP-Chip Data Production and Analysis

Microarrays were scanned using an Axon 4000B scanner (Axon Instruments, Foster City, CA), and the images were analyzed using GenePix 5.0. Each experiment was done in triplicate. Normalization and data analyses were not only carried out as described but also with a lower statistical cut-off value (Median Percentile Rank of 0.7 instead of 0.9) to decrease the selection stringency of regions showing significant fold-enrichment (Robine *et al*., 2007). Binding data were obtained with cells in YPD, YPA, and SPII at 4 and 8 h after initiation of meiosis. Cyanine (Cy)3/Cy5 and Cy5/Cy3 dye swap array data sets obtained with YPD cultures only were not averaged to determine the influence of the labeling reaction on the data output.

RNA Isolation and cRNA Target Synthesis

Culture conditions and one-channel microarray hybridization protocols were carried out as published with a few modifications. cRNA target molecules were prepared from 50-ml cultures at 3–5 × 10^7 cells/ml. Samples were hybridized to yeast S98 GeneChips (Affymetrix, Santa Clara, CA) that contain probes for ~6400 transcripts (http://www.affymetrix.com/). Fifteen micrograms of yeast total RNA was purified using RNeasy mini-spin columns (QIAGEN, Hilden, Germany) by using standard protocols provided by the manufacturer. The cell pellets were resuspended in RLT buffer (QIAGEN) and lysed by shearing in a 2-ml syringe. Supernatant (600 μl) was mixed with 600 μl of 70% ethanol, loaded onto an RNeasy column, washed, and eluted in 100 μl of double-distilled water. The total RNA quality was monitored using RNA Nano 6000 Chips processed with the 2100 BioAnalyzer (Agilent Technologies, Palo Alto, CA). Biotin labeling of RNA was done as outlined in the Expression Analysis Technical Manual with minor modifications. Single-stranded cDNA was synthesized by mixing 13 μg of total RNA with oligo(dT) and incubating the reaction mix with SuperScript II reverse transcriptase (Invitrogen) at 42°C for 1 h. After synthesis of the second cDNA strand using the Superscript double-stranded cDNA Synthesis kit (Invitrogen), the material was extracted with phenol-chloroform-isoamyl alcohol and precipitated with 0.5 volumes of 7.5 M ammonium acetate and 2.5 volumes of ethanol. The cDNA was used for an in vitro transcription reaction by using the BioArray high yield RNA transcript labeling kit T7 (Enzo Diagnostics, New York, NY) to synthesize cRNA in the presence of biotin-conjugated uridine 5′-diphosphate and cytidine 5′-triphosphate analogs. Approximately 50 μg of cRNA was purified over RNeasy Mini-Spin columns and analyzed again on RNA Nano 6000 Chips. The cRNA targets were incubated at 94°C for 35 min, and the resulting fragments of 50–150 nucleotides were again analyzed with RNA Nano 6000 Chips. All synthesis reactions were carried out in a PCR machine (T1 thermocycler; Biometra, Göttingen, Germany) to ensure optimal temperature control.

GeneChip Hybridization and Scanning

Hybridization cocktails (220 μl) containing heat-fragmented and biotin-labeled cRNA at a concentration of 0.05 μg/μl were injected into GeneChips and incubated at 45°C on a rotator in a hybridization oven 640 (Affymetrix) overnight at 60 rpm. The arrays are washed and stained with a streptavidin-phycoerythrin conjugate (Invitrogen). To increase signal strength, a standard antibody amplification protocol was used (EukGE-WS2v4; see Affymetrix Expression Analysis Manual). The S98 GeneChips were processed with a GeneArray Scanner 300 7G (Affymetrix) as described previously (Chalmel *et al*., 2007).

Microarray Data Processing and Statistical Analysis

Raw data were preprocessed (background adjustment, normalization, and summarization of probe sets) by using the Robust Multiarray Analysis package from BioConductor as described in Schlecht *et al*. (2004). First, probe sets for which we observed a signal equal or >100 (empirical conservative background threshold) in at least one condition were identified. Among those, differentially expressed probe sets were identified by analysis of variance. Genes were filtered using a p value <0.005 and a SD >0.3.

Cluster Analysis

Among the probe sets we identified those that were clearly associated with predicted genes, thus eliminating cases related to SAGE data and TY-elements for which probes are present on the S98 GeneChip. Genes identified as differentially expressed were then clustered using the k-means algorithm. Note that because of this approach, the sum of all genes in YPD and YPA clusters 1–3 shown in Figure 4D, clusters 4 and 5 shown in Supplemental Figure 5, and in SPII clusters shown in Figure 7B is smaller than the number indicated in the Venn diagram in Figure 4B.

Gene Ontology (GO) Analysis

Expression clusters were searched for enrichment of functions using the Annotation, Mapping, Expression and Network (AMEN) analysis tool (see SourceForge at http://sourceforge.net/projects/amen/), a new array data analysis and visualization software package (Chalmel and Primig, 2008). A specific annotation term was considered as enriched in a group of coexpressed genes if the p value was <0.005 and the number of genes in this cluster showing this annotation was >5. The results are output in a color-coded graph that facilitates the interpretation of expression patterns and their functional significance.

MIAME Compliance

CEL feature level data files and transcript level text files corresponding to rich medium (YPD), presporulation medium (YPA), and sporulation medium (SPII) samples are available via the EBI ArrayExpress public data repository at http://www.ebi.ac.uk/arrayexpress/under accession number E-TABM-291. Genome-wide DNA binding data are available via E-MEXP-1439.

RESULTS

abf1-1 ts Mutant Cells Fail to Undergo Normal Cytokinesis

Haploid *abf1-1* cells grow slowly at 30°C, become very large, form elongated buds, and arrest growth at several steps in the cell cycle when shifted to 37°C (Rhode *et al*., 1992). Homozygous diploid *abf1-1* mutant cells show similar temperature-dependent growth both on solid (Figure 1A) and in liquid rich medium (Figure 1C). This effect is complemented in cells containing a single-copy plasmid bearing a wild-type copy of *ABF1* controlled by its native promoter (Figure 1A, bottom row). Diploid strains heterozygous for *ABF1* grow both at the permissive and restrictive temperatures (Figure 1B, top), which is likely due to Abf1 being an abundant protein (Planta *et al*., 1995; Ghaemmaghami *et al*., 2003). However, *MAT*a/α cells containing only one *abf1-1* allele show a severe growth phenotype at the semipermissive temperature of 30°C (Figure 1B, top), indicating a dosage effect because diploid cells that contain two *abf1-1* alleles display only a mild phenotype (Figure 1A, middle). As expected, diploid strains that contain a wild-type copy of *ABF1* under the control of a galactose-inducible promoter and an endogenous wild-type or *abf1-1* mutant allele grow on rich medium containing galactose at the semipermissive temperature (Figure 1B, bottom). Note that the galactose-dependent induction of *ABF1* only partially complements the Abf1-1 phenotype at 37°C (Figure 1B, bottom). The GAL-Abf1 allele is a *priori* fully functional because the *GAL1-GAL10* intergenic region fused to a full-length *ABF1* locus can complement an *ABF1* gene deletion in haploid (Goncalves *et al*., 1992) and diploid cells (our own observation). However, overexpression of *ABF1* is toxic under certain conditions and additional heat stress may therefore result in partial growth inhibition (Donovan *et al*., 1998).

A detailed morphological examination revealed no difference between wild-type and mutant cells at the permissive temperature (Figure 1, D and E, left) of 25°C. As opposed to that, mutant cells grown at the semipermissive temperature of 30°C accumulated bodies of more than three unseparated and mostly unbudded enlarged cells (middle). This effect was also observed when mutant cells were cultured at 37°C, albeit at a lesser degree, because cells stop budding at that temperature (right). Together, these data indicate a dose-dependent growth effect of the *abf1-1* mutant allele in diploid cells and suggest a novel role for Abf1 in the regulation of cytokinesis.

The abf1-1 ts Mutant Is Sporulation Deficient at the Permissive Temperature

Previous work showed that normal expression of genes specifically transcribed during meiotic development required a functional Abf1 upstream activation sequence (UAS) target site (Prinz *et al*., 1995; Gailus-Durner *et al*., 1996; Ozsarac *et al*., 1997; Pierce *et al*., 1998). To directly test the role of the Abf1 protein in meiotic gene expression, diploid strains containing one wild-type or mutant *abf1-1* allele together with a GAL1-10-*ABF1* fusion, respectively, were constructed. This was done for two reasons: first, we sought to outcross the Abf1-1 allele into a different genetic background because the original isogenic W303 wild-type strain sporulated only very poorly, making it difficult to assess the effect of the mutated allele (Schlecht and Primig, unpublished observation). Second, we expected a strain containing only one transcriptionally active *abf1-1* temperature-sensitive allele to be suitable for analysis of meiosis at semipermissive conditions (28–30°C) because this process is inhibited by temperatures >34°C (Simchen, 1974).

Using fluorescence-activated cell sorting to measure the DNA content of cells, we determined that the *abf1-1* mutant strain was able to undergo premeiotic DNA replication with the same kinetics as the wild-type control at all three temperatures permissive for meiotic development tested (25, 28, and 33°C) (Figure 2A). This is in keeping with the fact that Abf1-1 does not affect transition through the mitotic S phase (Rhode *et al*., 1992). As expected, both strains failed to initiate premeiotic DNA replication at 37°C (Figure 2A). Next, we cultured the *abf1-1* strain at 25 and 28°C to ask whether temperatures still allowing for mitotic growth (permissive/semipermissive conditions) would impair the onset of meiotic M phase. To test this, the accumulation of bi- and tetranucleate cells as well as the formation of asci was monitored in wild-type and mutant cells. In a diploid strain containing one *abf1-1* allele, the efficiency of meiotic development was decreased at 25°C, severely reduced at 28°C, and abolished at 33°C, whereas a strain containing one wild-type allele sporulated normally at all permissive temperatures. Neither of the strains was able to enter meiotic M phase at 37°C (Figure 2B). These results show a role for the Abf1 protein in controlling the onset of meiotic M phase and spore development, which is coherent with previous reports on the role of its target sites in meiotic promoters.

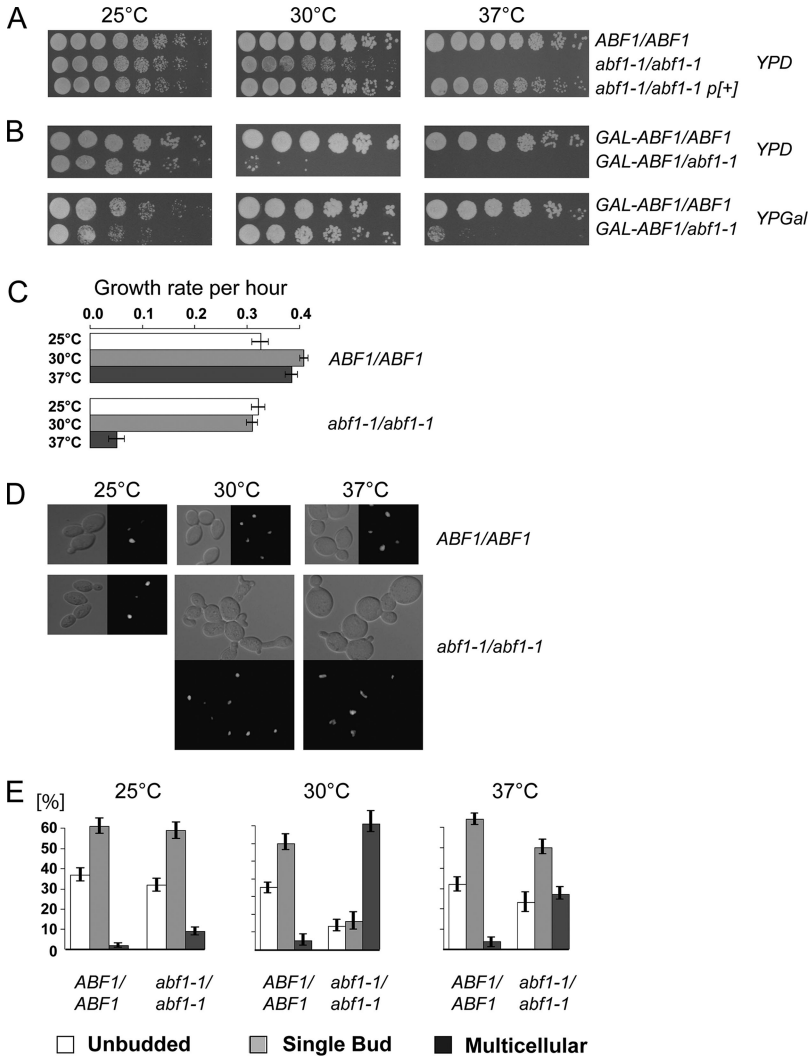

Figure 1. Growth properties of diploid *ABF1* wild-type versus *abf1-1* mutant strains. (A) Shown are serial fivefold dilutions of diploid wild-type (*ABF1/ABF1*; top), mutant (*abf1-1/abf1-1*; middle), and mutant cells transformed with a plasmid containing *ABF1* (*abf1-1/abf1-1* p[+]; bottom), grown for 2 d on YPD plates at the temperatures indicated. (B) Dilutions are given of an *ABF1*/abf1 heterozygous or abf1/abf1 homozygous strain containing an *ABF1* transgene fused to a galactose-inducible promoter as indicated, grown on YPD (top) or YPGal (bottom). (C) Growth rate of diploid wild-type (*ABF1/ABF1*) and mutant (*abf1-1/abf1-1*) strains in liquid YPD during 9 h at the temperatures indicated. Mean values from three independent experiments are shown. The bars represent the SD. (D) Cell morphology by differential interference contrast (DIC) and nuclear staining (DAPI) of wild-type and mutant strains at 25, 30, and 37°C as indicated. (E) Quantification of a cell separation defect in the *abf1-1* background. Cells were incubated at 25, 30, and 37°C during 4 h and the percentage of unbudded cells (white bar), cells with a single bud (light gray), and multicellular bodies (dark gray) was plotted on the *y*-axis against the wild-type and mutant strains on the *x*-axis. Mean values from three independent experiments are shown. Bars represent the SD.

The data also demonstrated that the *abf1-1* allele is a suitable tool for identifying not only mitotic but also meiotic Abf1 target genes via expression profiling at temperature conditions that impair Abf1-1 activity without inhibiting the meiotic process itself. Therefore, we set out to define genes directly controlled by Abf1 by validating target site predictions with genome-wide in vivo DNA binding assays and microarray profiling of wild-type versus temperature-sensitive mutant *abf1-1* strains at permissive, semipermissive, and restrictive conditions.

Computational Prediction of Abf1 Binding Sites Reveals Positional Similarity with Reb1

To identify putative Abf1 binding sites, a position-specific weight matrix was built by applying the PROCSE clustering algorithm (van Nimwegen *et al*., 2002) to experimentally verified Abf1 binding sites present in the promoters of genes such as *HOP1*, *CAR1*, and *SPR3* (Kovari and Cooper, 1991; Gailus-Durner *et al*., 1996; Ozsarac *et al*., 1997). Subsequently, we searched the multiple alignments of all intergenic regions in five related yeast species (Cliften *et al*., 2003) for matches to the Abf1 weight matrix, by using the MotEvo algorithm based on a Bayesian probabilistic approach that explicitly models the evolution of functional regulatory sites and nonfunctional intergenic DNA (Erb and van Nimwegen, 2006). We identified 1049 distinct intergenic regions that contain one or more putative Abf1 binding sites with significant probability. As expected, the weight matrix constructed from all predicted binding sites present in the budding yeast genome matches matrices obtained by in vitro selection of Abf1 binding sites (Mukherjee *et al*., 2004; Beinoraviciute-Kellner *et al*., 2005) and from high-throughput data (Kinney *et al*., 2007). Predicted motifs were found to be located preferentially ~100 base pairs upstream of the transcription start site, which is in keeping with a previous report (Yarragudi *et al*., 2007). Among >75 other transcription factors, only Reb1 binds to target sites that show a similar positional bias (Erb and van Nimwegen, 2006). Although Reb1 and Abf1 bind very different sequence motifs, both are general regulatory factors that enhance transcription by displacing nucleosomes (Lascaris *et al*., 2000; Angermayr *et al*., 2003; Yarragudi *et al*., 2004; Raisner *et al*., 2005).

Abf1 Displays Partially Distinct in Vivo DNA Binding Patterns during Mitosis and Meiosis

We next monitored Abf1/DNA interaction during mitotic growth in the presence of glucose (fermentation) and acetate (respiration) and during early and middle stages of meiotic development in diploid SK1, a strain we had previously used for growth and sporulation experiments (Primig *et al*.,

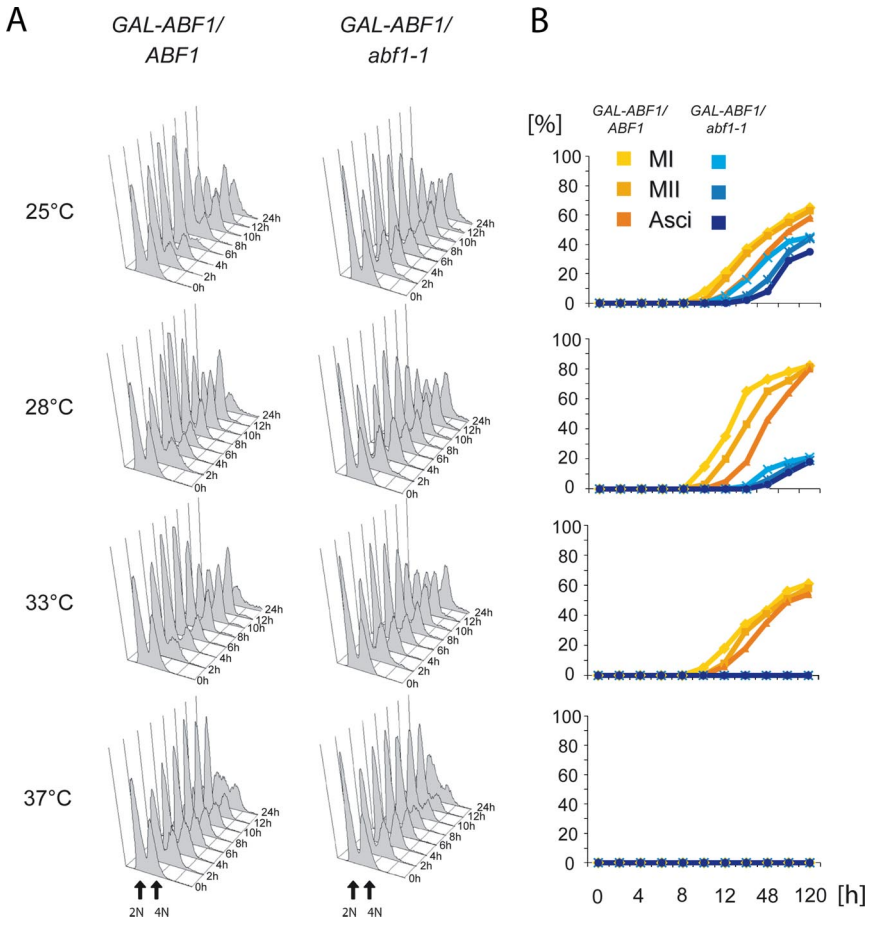

Figure 2. Determining meiotic landmark events in *ABF1* versus *abf1-1* strains. (A) Fluorescence-activated cell sorting analysis of premeiotic DNA replication in hetero- or homozygous abf1 deletion strains containing a GAL-*ABF1* construct at different temperatures and at the time points indicated. The DNA content of G1 and G2 cells is given as 2N and 4N. (B) Sporulation properties of strains containing one wild-type or mutant allele as indicated. The percentage of cells undergoing meiosis I, meiosis II, and ascus formation at the temperature indicated are plotted on the *y*-axis against time points on the *x*-axis from 0 to 120 h. Data from wild-type versus mutant alleles are color coded as given in the legend.

2000). Tagging Abf1 with a C-terminal HA epitope decreased sporulation efficiency and spore viability (our unpublished data). Therefore, we raised a polyclonal anti-Abf1 antibody against a 60-amino acid fragment between the DNA binding domains. The serum was shown to recognize the antigen (Supplemental Figure 1A) and the HA-tagged Abf1 expressed from its native promoter and Abf1 under the control of a galactose-inducible promoter (Supplemental Figure 1B). The result was confirmed by restaining the blot with a monoclonal antibody against the HA epitope (Supplemental Figure 1C). We next validated the Abf1 serum in an electrophoretic mobility antibody supershift assay by using an oligonucleotide probe containing the *HOP1* UAS. The free probe migrated as a single band (Supplemental Figure 1D, lane 1). On addition of a protein extract from mitotic cells, a slowly migrating complex was observed (lane 2) and found to be abolished in the presence of a molar excess of unlabeled $HOP1_{UAS}$ and $UME6_{UAS}$ wild-type (lanes 3 and 5) but not UAS mutant probes (lanes 4 and 6). No effect was observed upon addition of an antibody against Ndt80 (lanes 7–9), whereas the anti-Abf1 serum shifted the Abf1/DNA complex in a concentration-dependent manner (lanes 10–12). To test the ability of the Abf1 antibody to recognize the protein in vivo during mitotic growth, we performed qualitative chromatin immunoprecipitation control experiments that confirmed known binding activities to the *MCK1* (Harbison *et al.*, 2004) and *ZIP1* (Prinz *et al.*, 1995) promoters (Supplemental Figure 1E, top and middle). Note that no in vivo binding activity was observed in the *HOP1* promoter whose UAS element is thought to be bound by Abf1 (bottom) (Prinz *et al.*, 1995; Gailus-Durner *et al.*, 1996).

The genome-wide binding experiments using spotted microarrays covering ~13,000 intergenic sequences and open reading frames were done in triplicate (Figure 3A and Supplemental Figure 2A). Standard controls (dye-swap, mock immunoprecipitation, and input-overinput) were carried out to correct for systematic errors using cells cultured in YPD (Supplemental Figure 2B). A comparison of binding data from mitotic and meiotic cells revealed the upstream sequences of 1169 genes to be bound in three media by using nonstringent selection criteria (see *Materials and Methods*); a subset of these potential promoter regions such as i*MRPS18/*i*MCK1* and i*MSS4/*i*UME6* also contained at least one predicted binding motif (p value of 5.4×10^{-254}) (Figure 3B). Importantly, our data showed a significant overlap (p value of 2.1×10^{-149}) with a previous study that identified 458 Abf1 target promoters in haploid cells cultured in rich medium (Harbison *et al.*, 2004). Like in a qualitative chromatin immunoprecipitation assay (Supplemental Figure 1E), we did not observe any interaction of Abf1 with its target site in the *HOP1* promoter during mitosis or meiosis (Figure 3B, bottom right), whereas we show that the promoter of *ZIP1* is bound in vivo during growth and meiotic development (bottom left). It is noteworthy that binding to 82, 105, and 331 fragments was only detected during fermentation (YPD), respiration (YPA), or sporulation (SPII), respectively, indicating that the DNA binding affinity of Abf1 to some of its targets or their accessibility changes during these processes. Lists of genes whose promoters are detected as constitutively bound or specifically enriched during any of the conditions tested are available (Supplemental Table 1). We applied a less stringent selection procedure than a previous

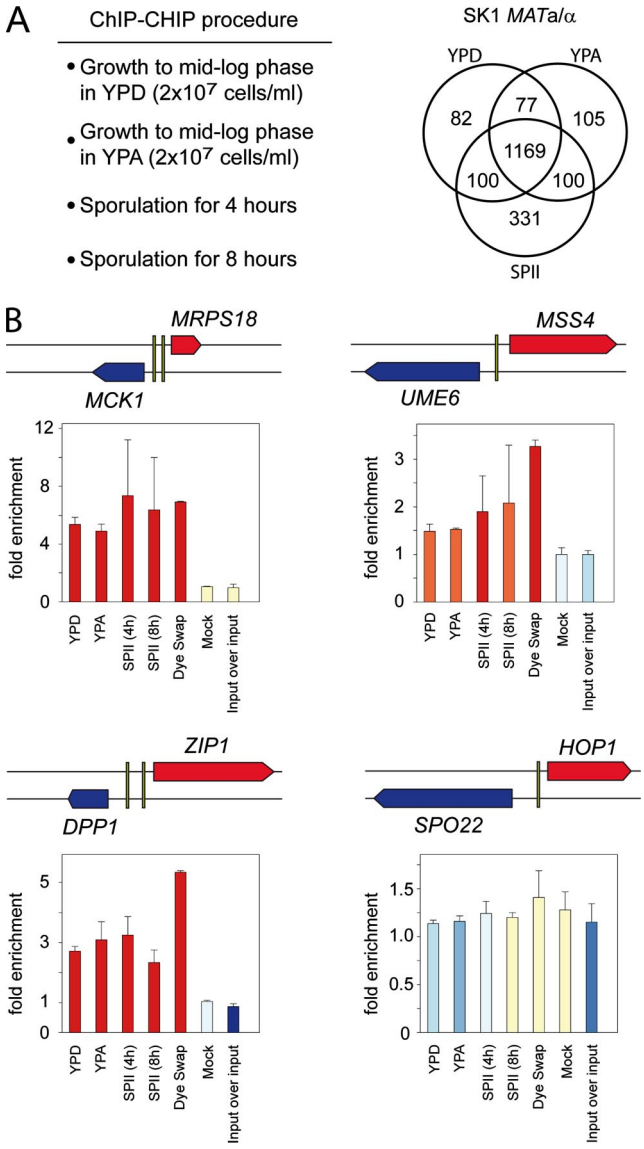

Figure 3. Genome-wide Abf1 in vivo binding assay. (A) Summary of the approach and Venn diagram of fragments found to be enriched above background in a diploid SK1 strain grown in rich medium with glucose (YPD) or acetate (YPA) or incubated for 4 and 8 h in sporulation medium (SPII). (B) Graphical display of four intergenic regions containing matches to UAS motifs (black vertical bars) and the corresponding genes on the top (red) and bottom (blue) strands. The fold-enrichment is plotted on the *y*-axis against experiments by using cells cultured in media as indicated. Sporulating cells were harvested 4 h (SPII 4h) and 8 h (SPII 8h) after induction of meiosis. Control experiments with cells cultured in YPD at 30°C were done using reversed fluorophor labeling (dye-swap), an unrelated antibody (mock), and no antibody (input over input). A color code indicates significant enrichment (red, orange) or background signals (blue, yellow).

study (Robine *et al.*, 2007; see *Materials and Methods*) because the binding data are integrated with results of motif prediction and expression profiling methods. Importantly, using the more selective filtration approach also reproducibly yields different binding patterns (Supplemental Figure 3, A and B).

Many promoter regions bound by Abf1 also seem to interact with other site-specific DNA binding regulators involved in metabolic functions (Gcn4 and Ino4), cell cycle regulation (Swi4 and Fkh1), chromatin remodeling (Cbf1 and Spt10), induction of pseudohyphal growth (Phd1), and the mitotic repression of meiosis-specific genes (Ume6 and Sum1) (Table 2). This is in keeping with the fact that Abf1 was often found to contribute to normal expression via chromatin opening rather than being the sole essential factor activating a promoter (Yarragudi *et al.*, 2004).

Table 2. Comparison of genome-wide DNA binding assays

Gene	Target genes (Harbison et al. 2005) ($p < 0.005$)	Overlap with this study	Significance of overlap
Abf1	468	387	2.06×10^{-149}
Ume6	244	113	7.24×10^{-11}
Gcn4	103	45	7.24×10^{-4}
Fkh1	239	86	0.00016
Swi4	218	78	0.00041
Ino4	123	46	0.00171
Phd1	131	47	0.00414
Spt10	8	5	0.00516
Cbf1	73	27	0.01300
Abt1	3	2	0.01748
Sum1	96	33	0.02454

Identification of Mitotic Abf1 Target Genes by Expression Profiling

Diploid wild-type and *abf1-1* mutant strains were cultured in rich medium containing glucose (YPD) or acetate (YPA) at the permissive (25°C) temperature until mid-log phase and then shifted to restrictive (37°C) conditions for 1 h before harvesting. Samples were analyzed in duplicate using high-density oligonucleotide microarrays containing probes covering ~6400 yeast protein coding loci (S98 GeneChips) (Figure 4A). Total RNA and cRNA quality was assessed using the BioAnalyzer and found to be excellent and very homogenous (Supplemental Figure 4A). Differentially expressed genes were filtered using SD and a permutation test as published and clustered using the k-means algorithm (Schlecht *et al.*, 2004). Expression clusters were searched for enriched functional annotation using data from the Gene Ontology consortium (www.geneontology.org/) and AMEN software (Chalmel and Primig, 2008).

In total, 3717 probe sets that map to 3214 unique protein-coding yeast genes representing ~47% of the transcripts detected by the S98 Affymetrix GeneChip were identified as being differentially expressed between wild-type and mutant strains in at least one condition tested. This fairly large gene output compared with previous studies is likely due to relaxed selection criteria (see *Materials and Methods*) and inclusion of three growth and developmental conditions (Miyake *et al.*, 2004; Yarragudi *et al.*, 2007). Three hundred twenty-one genes were detected in three media, whereas 626, 966, and 627 were filtered only in YPD, YPA, or SPII medium, respectively (Figure 4B). This does not necessarily reflect growth- or sporulation-specific regulation but rather a media-specific threshold effect (i.e., some genes are differentially expressed in two or all media, but the effect is strong enough to be detected by our filtration procedure only in one condition). We then grouped the genes into coregulated clusters and correlated transcriptional deregulation with the presence of a predicted binding motif and in vivo Abf1 promoter binding (Figure 4C).

The loci detected during fermentation in YPD (1798) and/or during respiration in YPA (2312) were separately

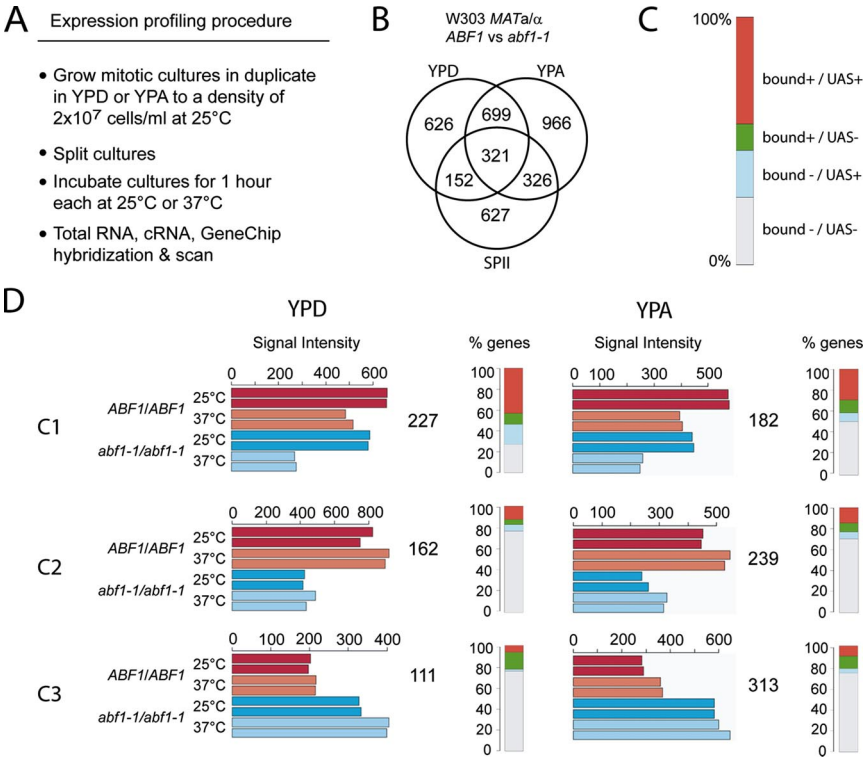

Figure 4. Identification of mitotic Abf1 target genes by using Affymetrix S98 GeneChips. (A) Outline of the approach. (B) Venn diagram of a comparative profiling experiment using diploid wild-type *ABF1* versus abf1-1 mutant strains compared at 25 versus 37°C (log-phase growth, mitosis) and at 28°C (6- and 10-h time points, meiosis). Genes detected in three media as indicated are given. (C) Color-coded bar diagram displaying differentially expressed genes whose promoters are bound and contain a UAS motif (red, bound+/UAS+), whose promoters are bound but lack a UAS motif (green, bound+/UAS−), whose promoters are not bound but do contain a UAS motif (blue, bound−/UAS+) and whose promoters are not bound and lack UAS (bound−/UAS−). (D) Overview of three different expression clusters (C1–C3) identified among genes in rich medium with glucose (YPD) or acetate (YPA). Diploid wild-type (*ABF1/ABF1*, red) and temperature-sensitive mutant strains (*abf1-1/abf1-1*, blue) are indicated. Median signal intensities are plotted against samples analyzed in duplicate at the temperatures shown. The total number of genes in each cluster is given. The gene content of clusters C1–C3 identified in YPD and YPA overlaps but is not identical. Percentages of genes falling into any of four categories outlined in C are shown.

organized into five expression clusters that turned out to be highly reproducible between media, including two that are temperature dependent (compare C1–C3 YPD vs. YPA in Figure 4D and C4 and C5 in Supplemental Figure 5). Genes in cluster 1 showed the lowest level of expression in mutant cells incubated at the restrictive temperature (37°C), which is the pattern we expected to find. Importantly, this cluster is highly enriched for loci whose promoters are bound by Abf1 and/or contain a predicted binding motif (73% in YPD and 56% in YPA). Moreover, it contains known Abf1 targets reported in molecular biological work (*ARO3*; Kunzler *et al.*, 1995) or expression studies (*TRP3*; Martens and Brandl, 1994). GO term analysis of YPD data shows that this cluster is enriched for genes involved in ribosome biogenesis and assembly ($p = 4.5 \times 10^{-4}$; 23 genes observed, 11 expected) and rRNA processing ($p = 1.4 \times 10^{-4}$; 20/8) (Figure 5A). This confirms previous reports that Abf1 is important for protein translation and amino acid biosynthesis (Mager and Planta, 1991). Furthermore, we find cellular localization ($p = 10^{-4}$; 43/24), protein targeting ($p = 2.3 \times 10^{-5}$; 24/10) and protein transport ($p = 2.2 \times 10^{-4}$; 34/18) as well as cytokinesis ($p = 6.6 \times 10^{-3}$; 11/5). The latter category includes genes required for budding (*BUD9*, *BUD31*, *GIC2*, *PWP2*, and *RAX2*), actin cytoskeletal organization and cell wall morphogenesis (*END3*, *PIK1*, and *SUN4*), and septation (*CDC3* and *CDC10*). YPA cluster 1 data yield for example metal ion transport ($p = 5.1 \times 10^{-6x}$; 12/3) and lipid metabolic process ($p = 5.3 \times 10^{-5}$; 20/8) (Figure 5B). Note that we display only enriched GO terms specific for genes in the YPA cluster to avoid partial redundancy with the YPD cluster.

We furthermore identified two clusters showing lower (cluster 2) or higher (cluster 3) expression in the mutant than in the wild-type strain at both the permissive and restrictive temperatures. This reveals an expression phenotype of *abf1-1* cells under conditions where normal growth and sporulation assays fail to indicate any pronounced defect. We note that *ABF1* fell into cluster 3 (increased transcription in the mutant at permissive and restrictive temperature), which confirms a previous observation that the protein regulates its own expression via a negative feedback loop (Halfter *et al.*, 1989; Miyake *et al.*, 2004). YPD cluster 2 is enriched for genes involved in DNA-mediated transposition ($p = 4.5 \times 10^{-64}$; 75/7), amine transport ($p = 1.7 \times 10^{-5}$; 11/2), and carboxylic acid transport ($p = 1.1 \times 10^{-6}$; 13/3). YPD cluster 3 is enriched for aerobic respiration ($p = 7.1 \times 10^{-4}$; 7/2), coenzyme biosynthetic process ($p = 9.5 \times 10^{-3}$; 5/1), and electron transport ($p = 1.4 \times 10^{-4}$; 8/2) (Figure 5A). YPA cluster 2 is, like its YPD counterpart, enriched in genes (albeit different ones) associated with DNA-mediated transposition ($p = 1.1 \times 10^{-8}$; 29/9) (Figure 5B). Interestingly, YPA cluster 3 is enriched for ribosome biogenesis and assembly ($p = 1.1 \times 10^{-26}$; 63/14), a term that is found in YPD cluster 1 (whose genes are expressed at the lowest level in the Abf1-1 mutant at 37°C). This may reflect different transcriptional regulation of ribosome biogenesis during fermentation and respiration (Schawalder *et al.*, 2004).

The remaining classes identified genes up- (cluster 4) or down-regulated (cluster 5) in both wild-type and mutant strains when cultured at the restrictive temperature (see Supplemental Figure 5). As expected, YPD cluster 4 is enriched in stress response ($p = 1.4 \times 10^{-8}$; 87/49) loci, including heat shock-inducible genes (*HSP12*, *HSP26*, *HSP30*, *HSP42*, *HSP78*, *HSP104*), whereas YPD cluster 5 is enriched for ribosomal genes (*DBP2*, *DBP9*, *LRP1*, *NIP7*, *NOP1*, *NOP12*, *RPL7B*, *RPL18B*, and *RPL36B*) repressed under heat shock conditions (Grigull *et al.*, 2004) (Figure 5, A and B). These results demonstrate that including wild-type and permissive temperature controls is crucial for the analysis and interpretation of expression data obtained with a temperature-sensitive mutant.

A

YPD cluster

Depleted p-value Enriched
1 0.95 0.05 1e-5 0

biological_process (35 terms)	5584	1 200	2 143	3 76	4 439	5 376
0006605 protein targeting	267	24 / 10	3 / 7	1 / 4	17 / 21	19 / 18
0051641 cellular localization	681	43 / 24	4 / 17	10 / 9	35 / 54	41 / 46
0015031 protein transport	508	34 / 18	3 / 13	4 / 7	34 / 40	27 / 34
0015992 proton transport	46	6 / 2	1 / 1	2 / 1	1 / 4	5 / 3
0015986 ATP synthesis coupled proton transport	37	5 / 1	1 / 1	2 / 1	1 / 3	5 / 3
0006403 RNA localization	128	11 / 5	0 / 3	0 / 2	3 / 10	12 / 9
0000910 cytokinesis	130	11 / 5	0 / 3	0 / 2	3 / 10	13 / 9
0006164 purine nucleotide biosynthetic process	73	7 / 3	5 / 2	2 / 1	4 / 6	10 / 5
0051170 nuclear import	74	7 / 3	1 / 2	0 / 1	1 / 6	3 / 5
0006364 rRNA processing	226	20 / 8	1 / 6	0 / 3	1 / 18	40 / 15
0042254 ribosome biogenesis and assembly	303	23 / 11	1 / 8	0 / 4	2 / 24	65 / 20
0006418 tRNA aminoacylation for protein translation	40	5 / 1	0 / 1	0 / 1	1 / 3	8 / 3
0009260 ribonucleotide biosynthetic process	67	7 / 2	2 / 2	2 / 1	5 / 5	11 / 5
0006520 amino acid metabolic process	248	20 / 9	15 / 6	3 / 3	40 / 20	28 / 17
0006313 transposition, DNA-mediated	265	0 / 10	75 / 7	0 / 4	10 / 21	0 / 18
0046942 carboxylic acid transport	99	4 / 4	13 / 3	1 / 1	4 / 8	3 / 7
0015837 amine transport	91	3 / 3	11 / 2	3 / 1	5 / 7	1 / 6
0009060 aerobic respiration	111	4 / 4	3 / 3	7 / 2	10 / 9	6 / 8
0009108 coenzyme biosynthetic process	96	6 / 3	2 / 3	5 / 1	12 / 8	9 / 7
0006118 electron transport	162	3 / 6	1 / 4	8 / 2	28 / 13	11 / 11
0006791 sulfur utilization	10	1 / 0	0 / 0	0 / 0	9 / 1	0 / 1
0009086 methionine biosynthetic process	29	1 / 1	0 / 1	0 / 0	14 / 2	2 / 2
0009607 response to biotic stimulus	72	4 / 3	3 / 2	3 / 1	21 / 6	0 / 5
0019344 cysteine biosynthetic process	12	0 / 0	0 / 0	0 / 0	7 / 1	0 / 1
0006950 response to stress	618	7 / 22	4 / 16	8 / 8	87 / 49	28 / 42
0009269 response to desiccation	8	0 / 0	0 / 0	0 / 0	5 / 1	0 / 1
0009414 response to water deprivation	8	0 / 0	0 / 0	0 / 0	5 / 1	0 / 1
0022618 protein-RNA complex assembly	139	6 / 5	0 / 4	0 / 2	1 / 11	35 / 9
0006413 translational initiation	46	4 / 2	0 / 1	0 / 1	0 / 4	17 / 3
0000154 rRNA modification	19	0 / 1	0 / 1	1 / 0	0 / 2	9 / 1
0006334 nucleosome assembly	21	0 / 1	0 / 1	0 / 0	0 / 2	7 / 1
0000054 ribosome export from nucleus	24	3 / 1	0 / 1	0 / 0	0 / 2	7 / 2
0006333 chromatin assembly or disassembly	125	7 / 5	2 / 3	2 / 2	2 / 10	17 / 8
0007096 regulation of exit from mitosis	22	1 / 1	0 / 1	0 / 0	0 / 2	5 / 2
0007093 mitotic checkpoint	22	0 / 1	0 / 1	0 / 0	1 / 2	5 / 2

B

YPA cluster

Depleted p-value Enriched
1 0.95 0.05 1e-5 0

biological_process (22 terms)	5584	1 145	2 188	3 252	4 162	5 164
0006826 iron ion transport	30	7 / 1	1 / 1	1 / 1	1 / 1	2 / 1
0030001 metal ion transport	95	12 / 3	1 / 3	1 / 4	4 / 3	6 / 3
0006694 steroid biosynthetic process	41	6 / 1	1 / 1	0 / 2	2 / 1	2 / 1
0006629 lipid metabolic process	308	20 / 8	10 / 10	4 / 14	13 / 9	8 / 9
0006812 cation transport	171	13 / 4	1 / 6	1 / 8	6 / 5	7 / 5
0006892 post-Golgi vesicle-mediated transport	70	6 / 2	0 / 2	1 / 3	2 / 2	1 / 2
0006631 fatty acid metabolic process	75	6 / 2	3 / 3	2 / 3	1 / 2	4 / 2
0006313 transposition, DNA-mediated	265	0 / 7	29 / 9	1 / 12	2 / 8	0 / 8
0005978 glycogen biosynthetic process	14	0 / 0	5 / 1	0 / 1	0 / 0	0 / 0
0006865 amino acid transport	80	1 / 2	8 / 3	1 / 4	3 / 2	3 / 2
0000082 G1/S transition of mitotic cell cycle	47	4 / 1	5 / 2	0 / 2	3 / 1	2 / 1
0042254 ribosome biogenesis and assembly	303	1 / 8	1 / 10	63 / 14	9 / 9	5 / 9
0006412 translation	390	13 / 10	4 / 13	70 / 18	5 / 11	14 / 12
0009451 RNA modification	62	0 / 2	0 / 2	16 / 3	1 / 2	0 / 2
0006400 tRNA modification	42	0 / 1	0 / 1	11 / 2	1 / 1	0 / 1
0006030 chitin metabolic process	19	3 / 1	0 / 1	0 / 1	5 / 1	0 / 1
0042546 cell wall biosynthetic process	61	1 / 2	0 / 2	0 / 3	6 / 2	1 / 2
0006486 protein amino acid glycosylation	77	0 / 2	1 / 3	1 / 4	8 / 2	7 / 2
0043413 biopolymer glycosylation	78	0 / 2	1 / 3	1 / 4	8 / 2	7 / 2
0009117 nucleotide metabolic process	160	3 / 4	8 / 5	5 / 7	2 / 5	13 / 5
0006769 nicotinamide metabolic process	39	2 / 1	4 / 1	0 / 2	0 / 1	5 / 1
0019362 pyridine nucleotide metabolic process	41	2 / 1	4 / 1	0 / 2	0 / 1	5 / 1

Figure 5. Biological Process GO term enrichment in mitotic expression clusters. (A) GO terms identified in five clusters from cells grown in YPD as given on top of the diagram. Rectangles contain bold numbers of enriched genes associated with a specific GO term as observed and expected. The total number of genes in the genome bearing a given GO term is shown. The numbers of genes bearing a GO term for each cluster are indicated at the top. Overrepresentation (red) and underrepresentation (blue) are color coded as shown in the scale bar (top left). (B) Data for gene clusters identified in YPA.

Abf1 Core Targets Include Multicomponent Factors Required for Cytokinesis

We identified 434 genes that were down-regulated in the Abf1-1 background during mitotic growth and/or meiotic development (cluster 1 genes). Among those, we found 157 core target genes whose promoters contained a predicted target motif, and they were bound by Abf1 in vivo. This group revealed (among other genes required for budding, actin cytoskeletal organization, and septation) *CDC3*, a member of the family of bud neck filaments required for growth and spore formation as a potential Abf1 target gene (Fares *et al*., 1996; for review, see Longtine *et al*., 1996; www.germonline.org/). Because absence of Cdc3 function causes a defect in cytokinesis and abnormal budding (Kim *et al*., 1991), we concluded that Abf1 might in part regulate bud formation and daughter cell separation by directly controlling expression of Cdc3. To confirm the chromatin immunoprecipitation experiment and to test whether the predicted $CDC3_{UAS}$ was indeed bound by Abf1, we performed an EMSA by using a radioactive oligonucleotide probe (Figure 6A, lane 1). A slowly migrating binding activity observed in a protein extract from growing wild-type cells (lane 2) was not shifted by the preimmune serum (lane 3), whereas an antibody against Abf1 did induce a supershift (lane 4) that was absent when a control antibody against Ndt80 was added (lane 5). The binding signal was abolished by an excess of unlabeled oligonucleotides containing wild-type $CDC3_{UAS}$ and $HOP1_{UAS}$ elements (lanes 6 and 8) but not by a mutated $HOP1_{UAS}$ (lane 7). These results indicate that Abf1 participates in the regulation of normal budding and cytokinesis by direct UAS-mediated transcriptional control of the critical septin *CDC3*. Next, we investigated whether formation of the septin ring structure necessary for daughter cell separation would be impaired in cells lacking fully functional Abf1. To this end, we visualized the structure by using Abf1 wild-type and mutant strains containing a Cdc3-green fluorescence protein fusion reporter gene. The data show that only the wild-type (Figure 6B, left) but not the mutant strain (right) is capable of forming the septin ring structure localized to the bud neck when cultured at the restrictive temperature of 37°C, whereas both strains form the septin ring at the permissive temperature of 25°C (Figure 6B as indicated). Thus, expression profiling, genome-wide and biochemical DNA binding assays, and cell biological data together suggest Abf1 to control septation via transcriptional regulation of *CDC3* expression. This finding is in keeping with the cytokinesis phenotype observed in *abf1-1* cells (Figure 1, D and E). We consider it unlikely, however, that suboptimal expression of Cdc3 alone is responsible for the defect, because other factors, such as Cdc10, also fail to reach normal expression levels in the mutant at the restrictive temperature (see YPD C1 and www.germonline.org/).

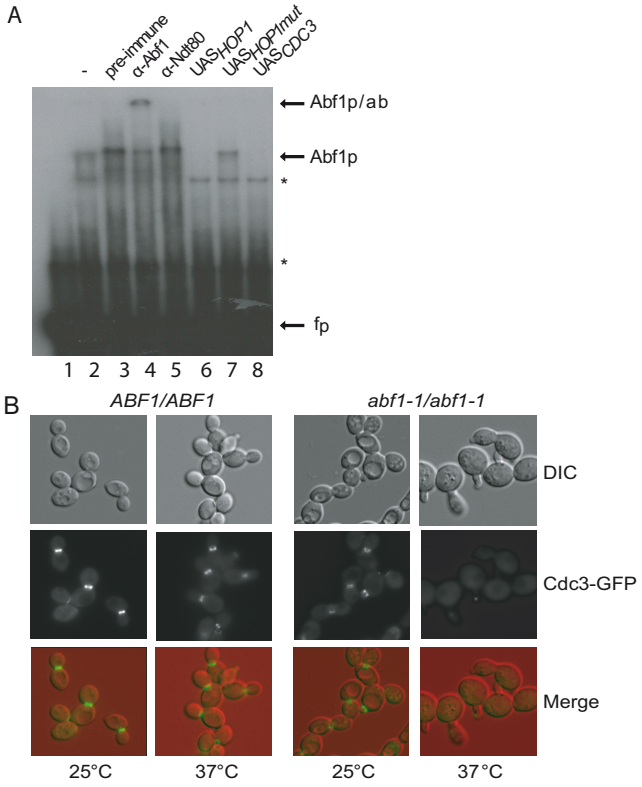

Figure 6. Abf1 binds to $CDC3_{UAS}$ and is required for septin formation. (A) Electrophoretic mobility antibody supershift assay by using a polyclonal anti-Abf1 antibody and a radioactive $CDC3_{UAS}$ probe. The free probe (lane 1) is followed by a binding activity present in an extract from cells cultured in YPD (lane 2). Preimmune serum (lane 3), Abf1 (lane 4, α-Abf1), and Ndt80 (lane 5, α-Ndt80) antibodies were diluted 1:30 and added to the binding reaction. A 100-fold molar excess of unlabeled wild-type (lane 6) and mutated (lane 7) $HOP1_{UAS}$ as well as wild-type (lane 8) $CDC3_{UAS}$ probes was added. Free probe (fp), a nonspecific band (*), and Abf1/DNA (Abf1p) and Abf1/antibody/DNA (Abf1p/ab) complexes are marked with arrows. (B) Fluorescence microscopic analysis of diploid wild-type (*ABF1/ABF1*) and mutant (*abf1-1/abf1-1*) cells containing a green fluorescent protein-tagged Cdc3. The strains were incubated in YPD at 25 and 37°C. The cell morphology (DIC, top) and GFP-signals (Cdc3-Gfp, middle) are shown individually and in an overlapping view (Merge, bottom).

Abf1 Controls Genes Involved in Inhibition of Meiosis, Spore Formation and Germination

Diploid strains containing one wild-type or Abf1-1 mutant allele were cultured in sporulation medium containing acetate and standard supplements (SPII) at the permissive temperature (25°C) until 5 and 9 h after induction of meiosis before they were shifted to 28, 33, or 37°C for 1 h (Figure 7A). Samples were analyzed in duplicate as described for the mitotic experiment (Supplemental Figure 4B). Note that only the meiotic samples harvested at 28°C were used for clustering (Figure 7B). Meiotic cluster 1 contained genes that failed to be induced to wild-type levels in the Abf1-1 mutant strain. As anticipated, the promoters of 40% of the genes in this cluster were bound by Abf1 and/or contained a predicted binding motif. The remaining expression clusters contained genes that were either repressed (cluster 2) or induced to various levels (clusters 3–5) during middle stages of sporulation in wild-type and mutant cells. All clusters showing unanticipated patterns contained a certain percentage of confirmed promoters (bound by Abf1 and/or predicted motif) and the level of induction observed in clusters 3–5 was indeed lower in the mutant strain than in the wild type. To rule out that different signal intensities were due to slower meiotic progression (hence, lower gene induction) by the mutant strain per se, we compared the induction profiles of known meiotic genes in Abf1 versus *abf1-1* cells at the permissive temperature of 28°C, and we found no substantial difference (Supplemental Figure 6A); this was observed for very early, early, middle, and mid-late genes (Supplemental Figure 6B). Meiotic expression clusters displayed no significantly enriched relevant GO terms; however, we identified genes essential for inhibition of meiosis (*APS2*, *PPH21*, *SET3*, and *UBR2*), synaptonemal complex (SC) formation

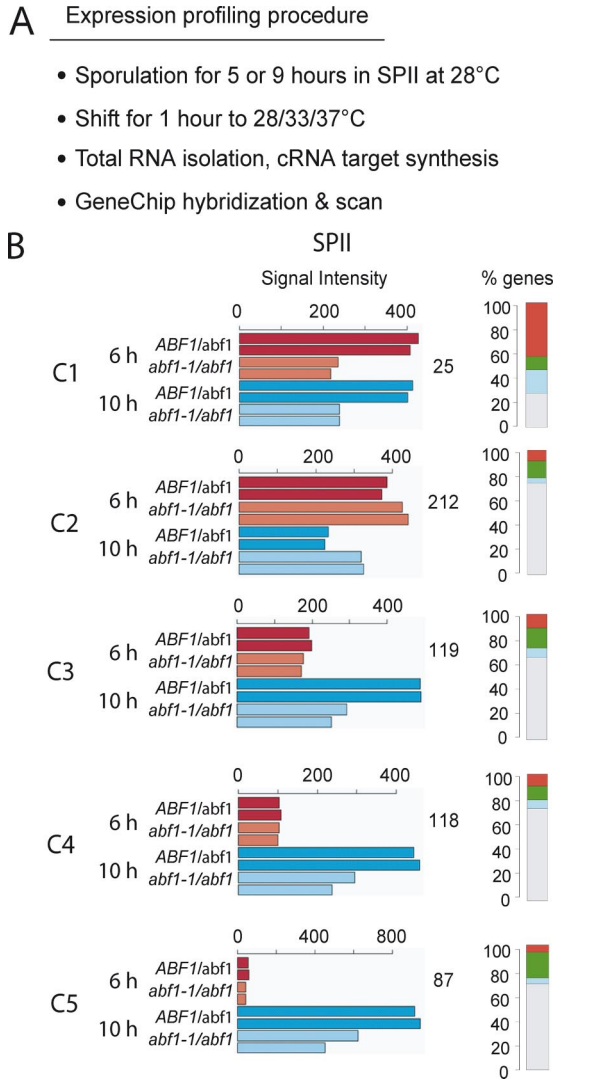

Figure 7. Identification of meiotic Abf1 target genes. (A) Outline of the approach. (B) Five expression clusters (C1–C5) identified among genes in sporulation medium at 28°C. Note that although C3-C5 seem rather similar, we empirically determined five clusters to be the number that identifies the largest percentage of genes in C1 confirmed by in vivo binding and presence of a putative target site in the promoter. Strains containing one wild-type (*ABF1*/abf1, red) and one mutant allele (*abf1-1*/abf1, blue) and a GAL-*ABF1* transgene are indicated. Median signal intensities are plotted against samples analyzed in duplicate at the time points shown. The total number of genes in a cluster is given. Percentages of genes falling into any of four categories outlined in Figure 4C are shown.

(*RED1* and *ZIP1*), sporulation (*CHS5*, *PEP12*, *SNF8*, *TAO3*, and *THR4*), and spore germination (*MRPL32*, *NFU1*, and *UBP6*) as Abf1 targets (Deutschbauer *et al.*, 2002; Deutschbauer and Davis, 2005).

Abf1 Binds to Meiotic Promoters during Mitosis and Meiosis

We next determined mitotic versus meiotic Abf1 promoter occupancy in the presence of a predicted motif for genes specifically expressed during meiosis to ask whether the protein bound only when a locus was actively transcribed. Abf1 was shown to interact with the upstream regions of early meiotic genes involved in control of the onset of meiosis (*IME4*), SC formation (*NDJ1*, *HFM1*, *RED1*, and *ZIP1*) and middle meiotic genes required for spore wall synthesis and maturation (*SPR3* and *SMK1*) under all conditions tested (Figure 8). This suggests that Abf1 is present at its site both during mitotic repression and meiotic induction of these promoters. In addition to this clear-cut situation, we also found meiosis-specific genes whose promoters were bound by Abf1 in at least one growth condition and during sporulation (*AMA1*, *DTR1*, *MAM1*, *MER1*, *PFS1*, *SMA1*, *SPO19*, *SPO73*, *SPS1*, *SPS100*, and *SWM1*) or only during meiotic development (*IME2*, *MUM1*, *MEK1*, and *SPO20*), although they contain no UAS (Figure 8).

A substantial number of potential target promoters lack a UAS element, whereas sequences that are bound by Abf1 in vivo do not seem to contain any novel conserved Abf1 motif. To test whether Abf1 could interact with base insertion or deletion variants of UAS that might elude our prediction algorithm, we determined their ability to compete a wild-type UAS motif in an EMSA. The results suggest that mutations changing the distance between the highly conserved 5′-TCA and 3′-ACG triplets abolished Abf1 interaction (Schlecht and Primig, unpublished observation). We conclude that Abf1 is unlikely to bind to mutant derivatives of its UAS target sites within the promoters that do not contain the known motif.

DISCUSSION

To fully understand the cellular functions of Abf1, it is necessary to identify its DNA binding patterns and its target genes during distinct stages of growth and development. In this study, we report a comprehensive genome-wide analysis of Abf1. It is based on probabilistic binding site prediction combined with an in vivo binding assay using mitotic and meiotic cells as well as expression profiling of growing or sporulating wild-type and temperature-sensitive mutant strains at both permissive and restrictive temperatures. Among 434 regulatory regions identified, 157 core promoters failed to be normally activated in the absence of fully functional protein (Abf1-1 at 37°C), were bound by Abf1 in vivo, and contained a predicted binding site. This group includes numerous genes not previously identified as Abf1 dependent. Although we found the majority of the promoters to be bound during growth (regardless of the carbon source) and spore development, a subset of regulatory elements were detected in only one or two of the conditions tested.

Correlating Abf1 Target Site Prediction, In Vivo Binding, and Target Gene Deregulation

Comparing computational and molecular biological methods reveals that motif prediction and the in vivo binding assay yield the most concordant results, whereas binding and expression profiling data show the smallest overlap in Abf1 (Supplemental Figure 7, A–C). We conclude that computational predictions of UAS motifs significantly conserved in related budding yeast species are a strong indicator of a functional binding site. Moreover, the experimental approach based on comparing wild-type to mutant alleles at the permissive and restrictive temperatures was yielding, because we identified a cluster of genes that showed the anticipated down-regulation in the mutant at 37°C (Figures 4D, C1 and 7B, C1). It is important to note that this cluster contains the highest percentage of genes (~50% in YPD, ~30% in YPA, and ~40% in SPII) where deregulation in the mutant is confirmed by in vivo binding to the upstream region and the presence of a predicted binding site in the

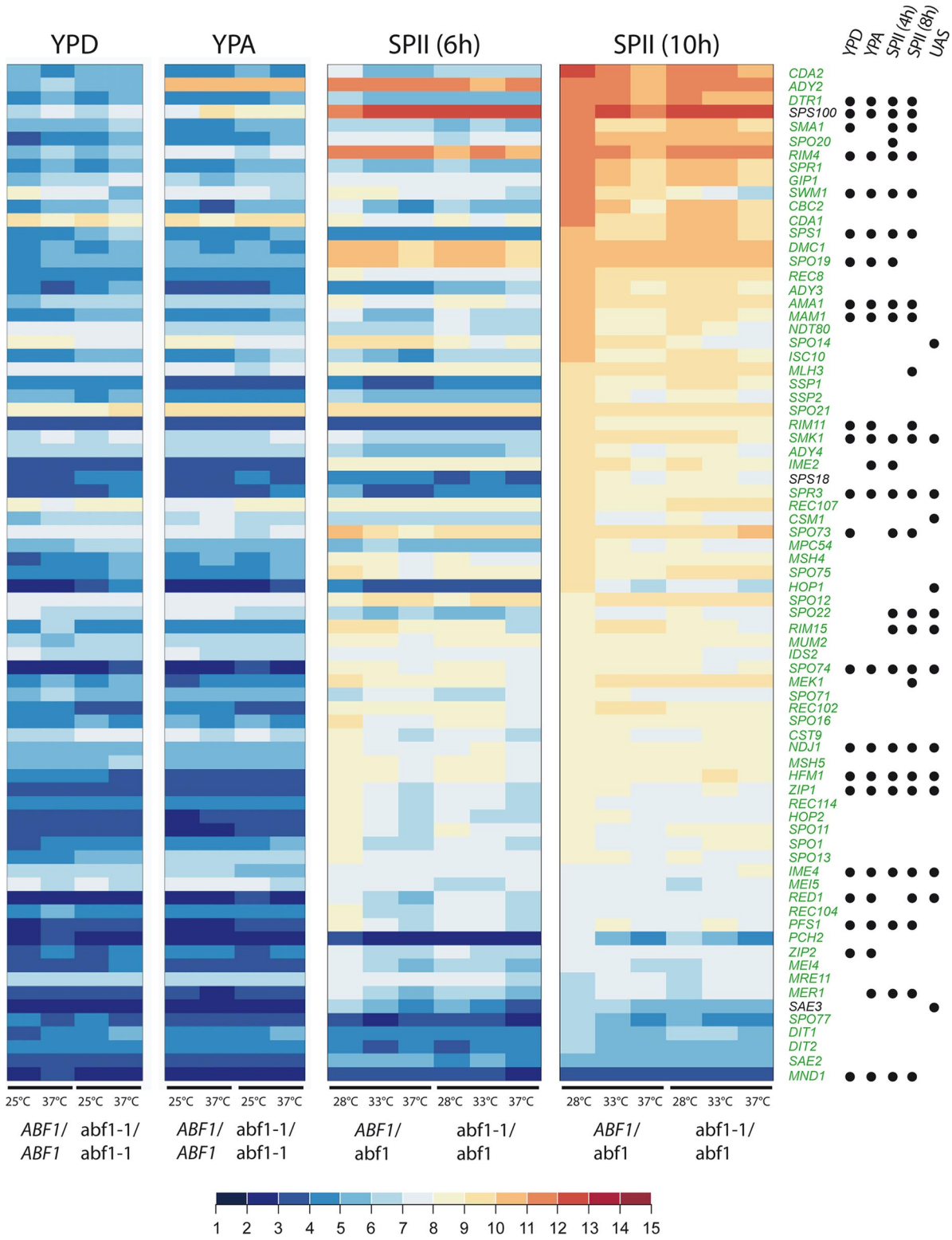

Figure 8. Abf1 control of essential meiotic genes. Color-coded heat maps displaying expression levels of meiotic genes in rich (YPD and YPA) and sporulation (SPII) media are shown. Homozygous wild-type (*ABF1*/*ABF1*) and mutant strains (*abf1-1*/*abf1-1*) and strains containing one wild-type (*ABF1*/abf1) or mutant allele (*abf1-1*/abf1) and a GAL-*ABF1* transgene are indicated. The temperatures are given at the bottom of the heat map. Dots mark genes whose promoters contain predicted binding sites (UAS) and/or are bound by Abf1 under different mitotic (YPD and YPA) and meiotic (SPII 4h, SPII 8h) conditions. Genes essential for meiosis and sporulation are shown in green. Log_2-transformed expression signal intensities are color coded as indicated in the scale bar.

promoter. However, the expected expression pattern is also observed when promoters are bound, although they lack a predicted binding site; when they are not bound, although they do contain a putative Abf1 binding site; and even in the absence of any detectable binding and a target site (Figure 4D). We do not believe that the protein interacts with other as yet unknown elements, because no novel conserved pattern was detected among the intergenic regions identified in the ChIP-Chip assay. It is possible that Abf1 has a nonspecific affinity for DNA during processes such as nucleotide excision repair (Reed *et al*., 1999) or mRNA transport (Hieronymus and Silver, 2003). This is in keeping with a recent in vitro analysis of the binding site of Abf1 that identified a pool of heterogeneous sequences not containing the UAS motif (Beinoraviciute-Kellner *et al*., 2005).

We have observed an unanticipated effect of the Abf1-1 allele at the permissive temperature that causes genes to show decreased (C2) or increased (C3) expression compared with the wild type. It is possible that these promoters contain low-affinity binding sites that Abf1-1 cannot interact with even at 25°C and that the overall expression of these genes mostly depends upon Abf1, so they are very sensitive to any perturbation. This is consistent with the finding that Abf1-1 fails to bind to its target site in vitro at room temperature (Rhode *et al*., 1992; Schlecht and Primig, unpublished observation). However, in most cases this effect seems to be indirect, because ~80% of the genes in these clusters have promoters that are not bound and lack a binding site.

The abf1-1 Allele as a Tool for Promoter Analysis

The *abf1-1* allele was used to study gene expression because the mutant cells stop growing and the Abf1-1 protein fails to bind to its target sites in vivo at 37°C (Miyake *et al*., 2004; Yarragudi *et al*., 2007). However, because it was observed that target genes continued to be expressed in the absence of detectable Abf1 binding at restrictive conditions it was postulated that the protein does not need to be continuously present on its target site once gene expression is activated (Schroeder and Weil, 1998). Another possibility is that Abf1-1 could still be able to at least partially interact with DNA at 37°C in the case of high-affinity binding sites or in a favorable protein network context. An assay more sensitive or different in its chemical nature than in vivo footprinting might reveal such residual binding. In this context, we note that FLAG-tagged Abf1-1 showed much reduced but not abolished binding to the *RPS28A* and *SPT15* promoters at the restrictive temperature when examined with a chromatin immunoprecipitation assay (ChIP; Yarragudi *et al*., 2007). We suspect that this binding signal might even be stronger in the case of the native protein because we found that HA-tagged Abf1 has a sporulation phenotype, indicating that the DNA binding capacity of tagged Abf1 might be reduced. Moreover, our ChIP assays using a polyclonal anti-Abf1 antibody seem to detect native Abf1-1 protein binding to the constitutive *UME6* promoter in YPD not only at 25°C but also at 37°C (Schlecht and Primig, unpublished observation).

Abf1 and Cytokinesis

Yeast *CDC3*, *CDC10*, *CDC11*, and *CDC12* septins were initially identified as mutants defective in bud-neck filament formation essential for cytokinesis (Hartwell, 1971). All septins except *CDC10* are cell cycle regulated and expressed or even highly induced during sporulation (Cho *et al*., 1998; Primig *et al*., 2000; www.germonline.org). The meiosis-specific septin *SPR3*, essential for normal spore development (Fares *et al*., 1996), is transcriptionally dependent upon Abf1 and Ndt80, the latter being a key regulator of middle meiotic genes (Ozsarac *et al*., 1997; Pak and Segall, 2002). Our finding that Abf1 is also likely to be directly required for the mitotic and meiotic expression of *CDC3* (and *CDC10*) is consistent with its role as a global regulator of septin-dependent functions such as cytokinesis and spore development. Moreover, it provides a partial explanation for the cytological and meiotic defects observed in the Abf1-1 mutant (Figures 1 and 6; Rhode *et al*., 1992). It is interesting to note that for mammalian septins such as SEPT3 (*CDC10* orthologue), SEPT10 (*CDC3*), and SEPT4 (*CDC12*), we have observed testicular expression reminiscent of the one found during mitotic growth and meiotic development in the case of their yeast orthologues (Schlecht *et al*., 2004; Chalmel *et al*., 2007). Such an expression pattern suggests an essential role for Septin genes during gametogenesis in mammals. Indeed, it was demonstrated that Sept4 $-/-$ male mice are infertile due to defective spermiogenesis, the postmeiotic process that leads to the production of spermatozoa (Ihara *et al*., 2005; Kissel *et al*., 2005).

Role of Abf1 during Meiosis

Abf1 was proposed to be a general activator of many early and middle meiotic genes, including some involved in synaptonemal complex formation (*HOP1*, *RED1*, and *ZIP1*) and spore wall formation (*SPR3*) based on mutation of its target site in the promoters of these genes (Vershon and Pierce, 2000). Unexpectedly, we detect Abf1 binding to the upstream regions of many meiotic genes (*AMA1*, *HFM1*, *IME4*, *MAM1*, *MND1*, *NDJ1*, *PFS1*, *SMK1*, *SPO74*, *SPR3*, *SPS1*, *SWM1*, and *ZIP1*) during both growth and development, suggesting that the presence of Abf1 on a meiotic promoter does not prevent its repression during mitosis.

Although ample evidence supports the notion that Abf1 binds and activates the *HOP1* promoter during meiosis (Prinz *et al*., 1995; Gailus-Durner *et al*., 1996), we and others (Harbison *et al*., 2004) failed to find supporting evidence by in vivo binding assays carried out using mitotic and meiotic cells. Perhaps Abf1 does not bind to the UAS_{HOP1} target site in living cells, hence, another protein with overlapping sequence specificity might fulfill an activating role at that UAS. An alternative explanation is that the Abf1 binding affinity to its target site in the *HOP1* 5′-upstream region is rather weak under all physiological conditions tested and therefore remains below our assay's threshold level of detection. This might be the case for a number of promoters that seem not to be bound, although they contain predicted target motifs.

Finally, we found no evidence for a role of Abf1 in the regulation of loci required for meiotic recombination (*SPO11*, *DMC1*, *REC104*, and *REC114*), chromosome cohesion (*REC8*) or control of the meiotic divisions (*SPO13*), although they are repressed during mitosis by Ume6 via its URS1 motif, which is often colocalized with the UAS of Abf1 (Williams *et al*., 2002). Recent results show that Ume6 is not converted to a coactivator by interaction with the inducer of meiosis Ime1, as thought previously, but rather it is destroyed in a Cdc20-APC/C–dependent manner soon after the onset of meiosis (Mallory *et al*., 2007). It seems therefore that meiotic activation mechanisms might be more diverse than previously thought, thus raising the question of which factor(s) in addition to Abf1 might be critically involved in the induction of many early meiotic genes.

ACKNOWLEDGMENTS

We thank T. Walther for critical reading of the manuscript, H. Leroy and A. Assi for GermOnline system administration, and T. Aust for production of the Abf1 antibody. We acknowledge initial help with array data production and analysis by R. Züst, M. Bellis, C. Niederhauser-Wiederkehr, and F. Chalmel. This project was supported by Swiss National Foundation grant no. 3100A0-105861 (to M.P.).

REFERENCES

Angermayr, M., Oechsner, U., and Bandlow, W. (2003). Reb1p-dependent DNA bending effects nucleosome positioning and constitutive transcription at the yeast profilin promoter. J. Biol. Chem. *278*, 17918–17926.

Beinoraviciute-Kellner, R., Lipps, G., and Krauss, G. (2005). In vitro selection of DNA binding sites for ABF1 protein from *Saccharomyces cerevisiae*. FEBS Lett. *579*, 4535–4540.

Borde, V., Lin, W., Novikov, E., Petrini, J. H., Lichten, M., and Nicolas, A. (2004). Association of Mre11p with double-strand break sites during yeast meiosis. Mol. Cell *13*, 389–401.

Chalmel, F., and Primig, M. (2008). The Annotation, Mapping, Expression and Network (AMEN) suite of tools for molecular systems biology. BMC Bioinformatics *9*, 86.

Chalmel, F. *et al*. (2007). The conserved transcriptome in human and rodent male gametogenesis. Proc. Natl. Acad. Sci. USA *104*, 8346–8351.

Cho, G., Kim, J., Rho, H. M., and Jung, G. (1995). Structure-function analysis of the DNA binding domain of *Saccharomyces cerevisiae* ABF1. Nucleic Acids Res. *23*, 2980–2987.

Cho, R. J. *et al*. (1998). A genome-wide transcriptional analysis of the mitotic cell cycle. Mol. Cell *2*, 65–73.

Cliften, P., Sudarsanam, P., Desikan, A., Fulton, L., Fulton, B., Majors, J., Waterston, R., Cohen, B. A., and Johnston, M. (2003). Finding functional features in *Saccharomyces* genomes by phylogenetic footprinting. Science *301*, 71–76.

Deutschbauer, A. M., and Davis, R. W. (2005). Quantitative trait loci mapped to single-nucleotide resolution in yeast. Nat. Genet. *37*, 1333–1340.

Deutschbauer, A. M., Williams, R. M., Chu, A. M., and Davis, R. W. (2002). Parallel phenotypic analysis of sporulation and postgermination growth in *Saccharomyces cerevisiae*. Proc. Natl. Acad. Sci. USA *99*, 15530–15535.

Donovan, S., Dowell, S., Diffley, J., and Rowley, A. (1998). The Practical Approach Series, New York: Oxford University Press.

Erb, I., and van Nimwegen, E. (2006). Statistical features of yeast's transcriptional regulatory code. In: IEE Proceedings of the First International Conference on Computational Systems Biology, 20–23 July 2006, Shanghai, China, 112–118.

Fares, H., Goetsch, L., and Pringle, J. R. (1996). Identification of a developmentally regulated septin and involvement of the septins in spore formation in *Saccharomyces cerevisiae*. J. Cell Biol. *132*, 399–411.

Futcher, B. (2002). Transcriptional regulatory networks and the yeast cell cycle. Curr. Opin. Cell Biol. *14*, 676–683.

Gailus-Durner, V., Xie, J., Chintamaneni, C., and Vershon, A. K. (1996). Participation of the yeast activator Abf1 in meiosis-specific expression of the HOP1 gene. Mol. Cell. Biol. *16*, 2777–2786.

Gattiker, A., Niederhauser-Wiederkehr, C., Moore, J., Hermida, L., and Primig, M. (2007). The GermOnline cross-species systems browser provides comprehensive information on genes and gene products relevant for sexual reproduction. Nucleic Acids Res. *35*, D457–D462.

Ghaemmaghami, S., Huh, W. K., Bower, K., Howson, R. W., Belle, A., Dephoure, N., O'Shea, E. K., and Weissman, J. S. (2003). Global analysis of protein expression in yeast. Nature *425*, 737–741.

Goncalves, P. M., Maurer, K., Mager, W. H., and Planta, R. J. (1992). Kluyveromyces contains a functional ABF1-homologue. Nucleic Acids Res. *20*, 2211–2215.

Grigull, J., Mnaimneh, S., Pootoolal, J., Robinson, M. D., and Hughes, T. R. (2004). Genome-wide analysis of mRNA stability using transcription inhibitors and microarrays reveals posttranscriptional control of ribosome biogenesis factors. Mol. Cell. Biol. *24*, 5534–5547.

Halfter, H., Muller, U., Winnacker, E. L., and Gallwitz, D. (1989). Isolation and DNA-binding characteristics of a protein involved in transcription activation of two divergently transcribed, essential yeast genes. EMBO J. *8*, 3029–3037.

Harbison, C. T. *et al*. (2004). Transcriptional regulatory code of a eukaryotic genome. Nature *431*, 99–104.

Hartwell, L. H. (1971). Genetic control of the cell division cycle in yeast. IV. Genes controlling bud emergence and cytokinesis. Exp. Cell Res. *69*, 265–276.

Hieronymus, H., and Silver, P. A. (2003). Genome-wide analysis of RNA-protein interactions illustrates specificity of the mRNA export machinery. Nat. Genet. *33*, 155–161.

Hochwagen, A., Wrobel, G., Cartron, M., Demougin, P., Niederhauser-Wiederkehr, C., Boselli, M. G., Primig, M., and Amon, A. (2005). Novel response to microtubule perturbation in meiosis. Mol. Cell. Biol. *25*, 4767–4781.

Ihara, M. *et al*. (2005). Cortical organization by the septin cytoskeleton is essential for structural and mechanical integrity of mammalian spermatozoa. Dev. Cell *8*, 343–352.

Kellis, M., Patterson, N., Endrizzi, M., Birren, B., and Lander, E. S. (2003). Sequencing and comparison of yeast species to identify genes and regulatory elements. Nature *423*, 241–254.

Kim, H. B., Haarer, B. K., and Pringle, J. R. (1991). Cellular morphogenesis in the *Saccharomyces cerevisiae* cell cycle: localization of the CDC3 gene product and the timing of events at the budding site. J. Cell Biol. *112*, 535–544.

Kinney, J. B., Tkacik, G., and Callan, C. G., Jr. (2007). Precise physical models of protein-DNA interaction from high-throughput data. Proc. Natl. Acad. Sci. USA *104*, 501–506.

Kissel, H., Georgescu, M. M., Larisch, S., Manova, K., Hunnicutt, G. R., and Steller, H. (2005). The Sept4 septin locus is required for sperm terminal differentiation in mice. Dev. Cell *8*, 353–364.

Kovari, L. Z., and Cooper, T. G. (1991). Participation of ABF-1 protein in expression of the *Saccharomyces cerevisiae* CAR1 gene. J. Bacteriol. *173*, 6332–6338.

Kunzler, M., Springer, C., and Braus, G. H. (1995). Activation and repression of the yeast ARO3 gene by global transcription factors. Mol. Microbiol. *15*, 167–178.

Lascaris, R. F., Groot, E., Hoen, P. B., Mager, W. H., and Planta, R. J. (2000). Different roles for abf1p and a T-rich promoter element in nucleosome organization of the yeast RPS28A gene. Nucleic Acids Res. *28*, 1390–1396.

Lee, T. I. *et al*. (2002). Transcriptional regulatory networks in *Saccharomyces cerevisiae*. Science *298*, 799–804.

Longtine, M. S., DeMarini, D. J., Valencik, M. L., Al-Awar, O. S., Fares, H., De Virgilio, C., and Pringle, J. R. (1996). The septins: roles in cytokinesis and other processes. Curr. Opin. Cell Biol. *8*, 106–119.

Luscombe, N. M., Babu, M. M., Yu, H., Snyder, M., Teichmann, S. A., and Gerstein, M. (2004). Genomic analysis of regulatory network dynamics reveals large topological changes. Nature *431*, 308–312.

Mager, W. H., and Planta, R. J. (1991). Coordinate expression of ribosomal protein genes in yeast as a function of cellular growth rate. Mol. Cell Biochem. *104*, 181–187.

Mallory, M. J., Cooper, K. F., and Strich, R. (2007). Meiosis-specific destruction of the Ume6p repressor by the Cdc20-Directed APC/C. Mol. Cell *27*, 951–961.

Martens, J. A., and Brandl, C. J. (1994). GCN4p activation of the yeast TRP3 gene is enhanced by ABF1p and uses a suboptimal TATA element. J. Biol. Chem. *269*, 15661–15667.

Miyake, T., Loch, C. M., and Li, R. (2002). Identification of a multifunctional domain in autonomously replicating sequence-binding factor 1 required for transcriptional activation, DNA replication, and gene silencing. Mol. Cell. Biol. *22*, 505–516.

Miyake, T., Reese, J., Loch, C. M., Auble, D. T., and Li, R. (2004). Genome-wide analysis of ARS (autonomously replicating sequence) binding factor 1 (Abf1p)-mediated transcriptional regulation in *Saccharomyces cerevisiae*. J. Biol. Chem. *279*, 34865–34872.

Mukherjee, S., Berger, M. F., Jona, G., Wang, X. S., Muzzey, D., Snyder, M., Young, R. A., and Bulyk, M. L. (2004). Rapid analysis of the DNA-binding specificities of transcription factors with DNA microarrays. Nat. Genet. *36*, 1331–1339.

Notredame, C., Higgins, D. G., and Heringa, J. (2000). T-Coffee: a novel method for fast and accurate multiple sequence alignment. J. Mol. Biol. *302*, 205–217.

Ozsarac, N., Straffon, M. J., Dalton, H. E., and Dawes, I. W. (1997). Regulation of gene expression during meiosis in *Saccharomyces cerevisiae*: SPR3 is controlled by both ABFI and a new sporulation control element. Mol. Cell. Biol. *17*, 1152–1159.

Pak, J., and Segall, J. (2002). Regulation of the premiddle and middle phases of expression of the NDT80 gene during sporulation of *Saccharomyces cerevisiae*. Mol. Cell. Biol. *22*, 6417–6429.

Parkinson, H. *et al*.. (2005). ArrayExpress–a public repository for microarray gene expression data at the EBI. Nucleic Acids Res. *33*, D553–555.

Pierce, M., Wagner, M., Xie, J., Gailus-Durner, V., Six, J., Vershon, A. K., and Winter, E. (1998). Transcriptional regulation of the SMK1 mitogen-activated protein kinase gene during meiotic development in *Saccharomyces cerevisiae*. Mol. Cell. Biol. *18*, 5970–5980.

Planta, R. J., Goncalves, P. M., and Mager, W. H. (1995). Global regulators of ribosome biosynthesis in yeast. Biochem. Cell Biol. *73*, 825–834.

Primig, M., Sockanathan, S., Auer, H., and Nasmyth, K. (1992). Anatomy of a transcription factor important for the start of the cell cycle in *Saccharomyces cerevisiae*. Nature *358*, 593–597.

Primig, M., Williams, R. M., Winzeler, E. A., Tevzadze, G. G., Conway, A. R., Hwang, S. Y., Davis, R. W., and Esposito, R. E. (2000). The core meiotic transcriptome in budding yeasts. Nat. Genet. *26*, 415–423.

Primig, M., Winkler, H., and Ammerer, G. (1991). The DNA binding and oligomerization domain of MCM1 is sufficient for its interaction with other regulatory proteins. EMBO J. *10*, 4209–4218.

Prinz, S., Klein, F., Auer, H., Schweizer, D., and Primig, M. (1995). A DNA binding factor (UBF) interacts with a positive regulatory element in the promoters of genes expressed during meiosis and vegetative growth in yeast. Nucleic Acids Res. *23*, 3449–3456.

Raisner, R. M., Hartley, P. D., Meneghini, M. D., Bao, M. Z., Liu, C. L., Schreiber, S. L., Rando, O. J., and Madhani, H. D. (2005). Histone variant H2A.Z marks the 5′ ends of both active and inactive genes in euchromatin. Cell *123*, 233–248.

Reed, S. H., Akiyama, M., Stillman, B., and Friedberg, E. C. (1999). Yeast autonomously replicating sequence binding factor is involved in nucleotide excision repair. Genes Dev. *13*, 3052–3058.

Rhode, P. R., Elsasser, S., and Campbell, J. L. (1992). Role of multifunctional autonomously replicating sequence binding factor 1 in the initiation of DNA replication and transcriptional control in *Saccharomyces cerevisiae*. Mol. Cell. Biol. *12*, 1064–1077.

Robine, N., Uematsu, N., Amiot, F., Gidrol, X., Barillot, E., Nicolas, A., and Borde, V. (2007). Genome-wide redistribution of meiotic double-strand breaks in *Saccharomyces cerevisiae*. Mol. Cell. Biol. *27*, 1868–1880.

Schawalder, S. B., Kabani, M., Howald, I., Choudhury, U., Werner, M., and Shore, D. (2004). Growth-regulated recruitment of the essential yeast ribosomal protein gene activator Ifh1. Nature *432*, 1058–1061.

Schlecht, U., Demougin, P., Koch, R., Hermida, L., Wiederkehr, C., Descombes, P., Pineau, C., Jegou, B., and Primig, M. (2004). Expression profiling of mammalian male meiosis and gametogenesis identifies novel candidate genes for roles in the regulation of fertility. Mol. Biol. Cell *15*, 1031–1043.

Schlecht, U., and Primig, M. (2003). Mining meiosis and gametogenesis with DNA microarrays. Reproduction *125*, 447–456.

Schroeder, S. C., and Weil, P. A. (1998). Genetic tests of the role of Abf1p in driving transcription of the yeast TATA box binding protein-encoding gene, SPT15. J. Biol. Chem. *273*, 19884–19891.

Simchen, G. (1974). Are mitotic functions required in meiosis? Genetics *76*, 745–753.

Stark, C., Breitkreutz, B. J., Reguly, T., Boucher, L., Breitkreutz, A., and Tyers, M. (2006). BioGRID: a general repository for interaction datasets. Nucleic Acids Res. *34*, D535–D539.

Tan, K., Shlomi, T., Feizi, H., Ideker, T., and Sharan, R. (2007). Transcriptional regulation of protein complexes within and across species. Proc. Natl. Acad. Sci. USA *104*, 1283–1288.

van Nimwegen, E., Zavolan, M., Rajewsky, N., and Siggia, E. D. (2002). Probabilistic clustering of sequences: inferring new bacterial regulons by comparative genomics. Proc. Natl. Acad. Sci. USA *99*, 7323–7328.

Vershon, A. K., and Pierce, M. (2000). Transcriptional regulation of meiosis in yeast. Curr. Opin. Cell Biol. *12*, 334–339.

Williams, R. M., Primig, M., Washburn, B. K., Winzeler, E. A., Bellis, M., Sarrauste de Menthiere, C., Davis, R. W., and Esposito, R. E. (2002). The Ume6 regulon coordinates metabolic and meiotic gene expression in yeast. Proc. Natl. Acad. Sci. USA *99*, 13431–13436.

Yarragudi, A., Miyake, T., Li, R., and Morse, R. H. (2004). Comparison of ABF1 and RAP1 in chromatin opening and transactivator potentiation in the budding yeast *Saccharomyces cerevisiae*. Mol. Cell. Biol. *24*, 9152–9164.

Yarragudi, A., Parfrey, L. W., and Morse, R. H. (2007). Genome-wide analysis of transcriptional dependence and probable target sites for Abf1 and Rap1 in *Saccharomyces cerevisiae*. Nucleic Acids Res. *35*, 193–202.

Zhang, L. V., King, O. D., Wong, S. L., Goldberg, D. S., Tong, A. H., Lesage, G., Andrews, B., Bussey, H., Boone, C., and Roth, F. P. (2005). Motifs, themes and thematic maps of an integrated *Saccharomyces cerevisiae* interaction network. J. Biol. *4*, 6.

Zhang, Z., and Dietrich, F. S. (2005). Mapping of transcription start sites in *Saccharomyces cerevisiae* using 5′ SAGE. Nucleic Acids Res. *33*, 2838–2851.

Zhu, J., and Zhang, M. Q. (1999). SCPD: a promoter database of the yeast *Saccharomyces cerevisiae*. Bioinformatics *15*, 607–611.